Current understanding of the mechanisms by which membrane-active peptides permeate and disrupt model lipid membranes

Sun, Delin; Forsman, Jan; Woodward, Clifford E.

Published in:
Current Topics in Medicinal Chemistry

DOI:
10.2174/1568026615666150812121241

2016

Current Understanding of the Mechanisms by which Membrane-Active Peptides Permeate and Disrupt Model Lipid Membranes

Delin Sun[1], Jan Forsman[2], and Clifford E. Woodward[1,*]

[1]School of Physical, Environmental and Mathematical Sciences, University of New South Wales, Canberra ACT 2600, Australia

[2]Theoretical Chemistry, Chemical Centre, Lund University, P.O. Box 124, S-221 00 Lund, Sweden

[*] To whom correspondence should be addressed. E-mail: c.woodward@adfa.edu.au.

ABSTRACT

Three classes of membrane active peptides (MAPs) are considered in this review: cell penetrating peptides (CPPs); anti-microbial peptides (AMPs), and amyloidal peptides. We summarize both experimental and theoretical results for several representative peptides in these different classes, which highlight commonalities in their interactions with model lipid membranes. While it is clear that no fixed set of mechanisms completely characterize any particular class of MAPs, there is certainly evidence that common mechanisms can be found within and between classes. For example, CPPs appear to undergo rapid translocation across lipid bilayers through small transient pores, which nevertheless appear not to cause persistent damage to membranes. On the other hand, AMPs also show evidence of rapid translocation, but associated with this, is membrane rupture to form large pores, which are subsequently stabilized by peptide adsorption to the pore edges. This disruption to the membrane is presumably responsible for cell death. Amyloidal peptides also show evidence of stable large pore formation, however, the mechanism for pore stabilization appears linked with their ability to form fibrils and prefibrillar aggregates and oligomers. There is some evidence that pores and membrane defects in fact act as nucleation sites for these structures. Where possible we have related the experimental and theoretical work to our own simulation findings in an effort to produce a comprehensive, albeit speculative picture for the mechanisms of action for this important group of peptides.

Keywords: Membrane active peptides; anti-microbial peptides; cell-penetrating peptides; amyloid peptides; lipid membrane; pore-formation

Graphical Abstract

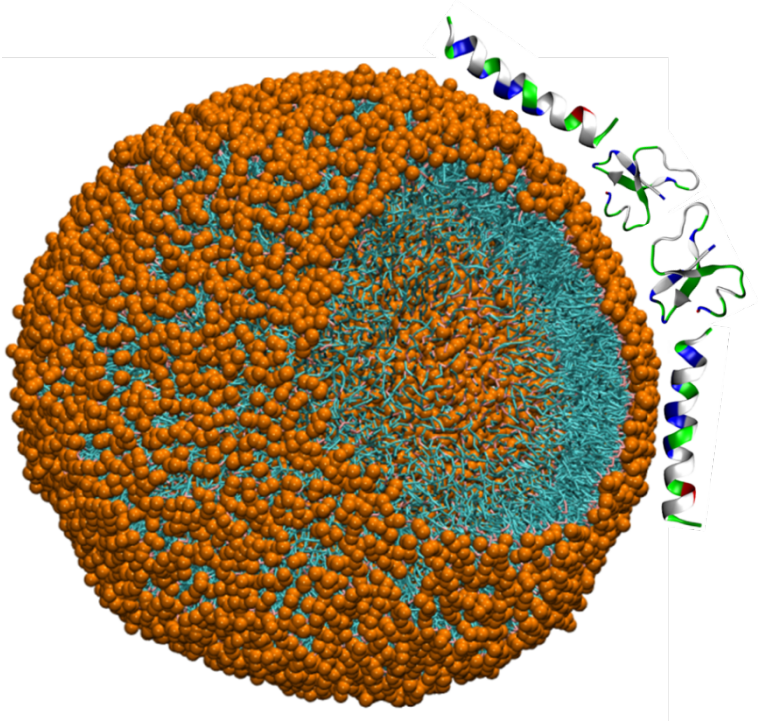

We review the modes of activity of three classes of membrane active peptides: cell penetrating; anti-microbial, and amyloid peptides.

Contents

1. INTRODUCTION

Membrane-active peptides (MAPs) comprise a wide range of short-sequenced proteins which possess the ability to readily permeate or even disrupt cell membranes in vivo. Prototypical examples of MAPs include cell penetrating peptides (CPPs), antimicrobial peptides (AMPs) and amyloid peptides. Deciphering the mechanisms of actions of these peptides in cell membranes is crucial for de novo development of safe and effective pharmaceutical delivery materials and therapeutic agents for human diseases like cancer, Alzheimer's disease, Parkinson disease, type II diabetes, viral infections, etc. Unfortunately, our present knowledge of the molecular process by which MAPs disrupt cell membranes is rather limited. This can be partially attributed to the complex structure of cell membranes.

The major components of cell membranes can be broadly subdivided into membrane lipids and membrane proteins. These are well organized in a bilayer structure and act cooperatively to carry out critical cellular activities. The intricacy of the cell membrane structure makes it very difficult to determine the underlying factors that are crucial to the activity of MAPs. In this regard, simplified model membranes with controllable membrane components have been particularly useful in unveiling important information regarding the modes of action of MAPs. Accumulating experimental and theoretical studies using model membrane systems have now established that the main target of MAPs is the membrane lipids (or phospholipids) [1-3]. These can be further divided into many groups based on the chemistry of the head group and the length and nature of the acyl chain. There are many different forms of model lipid membrane that have been used in experiments. The most common include lipid monolayers, supported lipid bilayers and lipid vesicles [4]. In molecular dynamics (MD) simulation studies, the lipid membrane is usually modeled as a small patch of lipid bilayer, containing around a hundred or more lipids. This has given rise to some concerns that these bilayer models are too rigid compared to relatively much larger cell membranes, so that large-scale dynamical structural fluctuations

in membranes are not observable in high-resolution atomistic simulations. This notwithstanding, these atomistic models can reasonably predict the interactions of amino acids with locally flat lipid membranes [5].

Investigating the mechanisms of membrane disruption by assorted peptides for different types of lipid membranes is essential to identifying the common molecular factors that potentially affect the activity of MAPs. Indeed, evidence from model lipid membrane studies has suggested that the structurally and chemically diverse MAPs may act analogously in the lipid membrane environment [6]. In this review article, we will summarize current knowledge about the membrane permeation and disruption actions of a few prototypical MAPs. Particular emphasis will be placed on the mechanisms that these MAPs utilize for the induction of pores in model lipid membranes.

2. CELL PENETRATING PEPTIDES

CPPs are short amino acid sequences which can traverse the cell membrane barrier without causing damage to the membrane integrity [7]. In biological experiments, CPPs have been widely employed to deliver into the cell cytoplasm therapeutic agents such as: drug molecules; DNA; SiRNA, and quantum dots [8,9]. However, the mechanism of the rapid permeation of CPPs through cell membranes still remains bewildering ever since their discovery more than two decades ago. CPPs are generally categorized into two classes, based on their amino acid compositions. They are:

(i) Arginine-rich cell penetrating peptides (ARCPPs). These consist of high contents of the cationic arginine residue. Common examples include the trans-activator of transcription (TAT) peptide, penetratin and oligoarginine.

(ii) Amphipathic cell penetrating peptides. These peptides are usually rich in hydrophobic residues and the cationic lysine residue. Transportan 10 (tp10) is the most studied amphipathic cell penetrating peptide.

2.1 TAT peptide

The ongoing debate surrounding the mechanism of membrane penetration used by ARCPPs began with the discovery of the TAT peptide (YGRKKRRQRRR) [10]. This peptide is highly charged due to the presence of six arginine and two lysine residues. Early biological experiments found that TAT could be internalized into cells at low temperatures, i.e., in the absence of cellular energy [10]. This finding suggested that cellular entry of TAT did not involve endocytotic mechanisms, but rather, direct (passive) membrane penetration was implied. However, from a thermodynamic viewpoint, the direct penetration of TAT peptide through a lipid bilayer is ostensibly extremely unfavorable, as could be inferred by the expected large Born energy required for transferring the cationic peptide from water to the lipid membrane interior. For example, the free energy cost for transferring just a single ion from water to the lipid bilayer center is estimated to be around 60 kJ/mol, which is approximately 30 times larger than typical thermal energies in the cytoplasm. However, the non-endocytotic translocation mechanism implied by those early experiments was seriously challenged by Richard and coworkers, who found that cell fixation led to the artificial uptake of TAT [11]. Instead, their experiments on live, non-fixated cells showed that the cellular uptake of TAT was significantly inhibited by incubation at low temperature, or by energy depletion [11]. The experimental results strongly supported endocytosis as a mechanism for the cellular internalization of TAT. Thereafter, accumulating experimental evidence has begun to highlight the role of endocytotic pathways in the cellular uptake of TAT, including macropinocytosis, clathrin-mediated endocytosis, and caveolae/lipid-raft-mediated endocytosis [12-14]. Notwithstanding this increasing experimental evidence, non-endocytotic and direct membrane permeation mechanisms

cannot be completely precluded. Indeed, *in vitro* and *in silico* studies on model lipid membranes have suggested that direct permeation of TAT through a bilayer can proceed via a peptide-induced membrane pore.

Synchrotron X-ray scattering (SAXS) experiments revealed that TAT peptide is able to transform a lamellar lipid membrane phase into a bi-continuous cubic phase, which is rich in saddle-splay structures possessing negative Gaussian curvature [15]. This transition was observed for membranes containing a high content of neutral phosphatidylethanolamine (PE) lipids together with anionic phosphatidylserine (PS) lipids and was thought to be stabilized with bidendate hydrogen bonds formed between guanidinium ions and lipid phosphate groups [15]. Though drastic membrane rearrangement is generally not seen in cellular uptake experiments, this lamellar to cubic phase transition is possibly related to the activity of TAT, especially given that toroidal membrane pores also have negative Gaussian curvature. Alternatively, it is known that PE lipids favor negative mean curvature in the bilayer and tend to interact very weakly with TAT peptide, while PS lipids will have strong interactions with cationic TAT peptides. These factors may lead to lipid separation in mixed PS/PE membranes, leading to a gel transition in the PE rich domain and subsequent compromise of the membrane [16]. The behavior of TAT in these types of membranes, suggests that this peptide is able to disrupt and penetrate bacterial and cancer cell membranes, which are rich in anionic and PE lipids.

Rapid pore formation induced by TAT also occurs in membranes devoid of PE lipids. For instance, fluorescence microscopy experiments conducted by Ciobanasu *et al.* showed that TAT peptide could induce nanoscale membrane pores in model bilayers containing PS lipids, phosphatidylcholine (PC) and cholesterol [17]. TAT was able to permeate these membranes without drastically altering the membrane morphology. The outer leaflet of mammalian cell membranes consists mainly of phosphatidylcholine (PC) lipids and cholesterol. On the question of how well TAT permeates model bilayers that mimic

mammalian membranes, there are conflicting answers from published *in vitro* experimental studies. Ciobanasu *et al.* found that TAT peptide did not permeate giant unilamellar vesicles (GUVs) containing PC lipid and cholesterol only, some anionic lipid was required for penetration [17]. While Piantavigna *et al*., using a combination of quartz crystal microbalance, scanning electrochemical microscopy and atomic force microscopy, found that TAT permeated large unilamellar vesicles (LGVs) consisting of 1, 2-dimyristoyl-*sn*-glycero-3-phosphocholine (DMPC) and cholesterol. Their AFM measurements revealed the formation of so-called "worm-holes" by TAT [18]. Somewhat consistent with these findings are X-ray and neutron reflectivity experiments conducted by Choi *et al*., who observed that membrane defects formed on a supported 1, 2-dipalmitoyl-*sn*-glycero-3-phosphocholine (DPPC) lipid bilayer upon TAT translocation [19].

There have been a number of MD simulation studies performed in an attempt to reveal how TAT peptide is able to permeate model lipid bilayers. As far as we are aware, the first MD simulation study of TAT interacting with the zwitterionic 1, 2-dioleoyl-*sn*-glycero-3-phosphocholine (DOPC) lipid bilayer was reported by Herce and García [20]. Their simulation results revealed the formation a transient pore in the membrane, allowing the TAT peptide to translocate. The relevant molecular factors for pore formation appeared to be the deep partitioning of TAT into the lipid bilayer and subsequent membrane thinning, coupled with strong electrostatic interactions between the peptide and the lipid heads on the distal leaflet of the bilayer. However, their simulations were later found to suffer from an artifact in the simulation setup, whereby a uniform neutralizing background gave rise to a charge imbalance across the bilayer with asymmetrically adsorbed peptide [21]. As confirmation of this effect, MD simulations by Yesylevskyy *et al*., using explicit neutralizing electrolyte did not show membrane pore formation by TAT in the DPPC lipid bilayer. However, TAT aggregation and membrane invagination, reminiscent of macropinocytosis, was observed instead [21]. A combined experimental and MD simulation study by

Akabori *et al*. suggests that the disruption of lipid membranes by TAT, characterized by disordered lipid packing and membrane thinning, may be an important preliminary step to pore formation [22]. Membrane thinning caused by TAT has also been found via neutron diffraction studies by Chen *et al* [23]. That work revealed very deep partitioning of TAT peptides in the glycerol regions of zwitterionic lipids, when the peptide concentration was high [23]. The embedding of TAT into the glycerol regions has also been verified with solid-state NMR experiments by Su *et al* [24]. However, TAT peptide deeply imbedded in this way has not been observed in atomistic MD simulations [22]. This could be an artifact of the force fields used or because the simulation time was insufficient to capture events, which likely occurs on a much longer timescale.

2.2 Penetratin

Penetratin (RQIKIWFQNRRMKWKK), another ARCPP, was also discovered two decades ago [25]. Its sequence corresponds to the third α-helix of the Antennapedia homeoprotein. As with TAT, much debate has occurred as to whether the cellular uptake of penetratin follows an endocytotic or non-endocytotic pathway [26-28]. Initially, it was thought that penetratin used the non-endocytotic mechanism, with inverse micelle formation playing a possible role [29]. While such a mechanism has not been validated experimentally, a coarse-grained simulation study by Kawamoto *et al*. supported the inverse micelle model [30]. However, the coarse-grained force field they used assumed unreasonably strong interactions between the peptide and lipid head groups. Atomistic simulations by Yesylevskyy *et al*. concluded that formation of inverse micelles within the membrane was unlikely [21]. Rather, it was found that, as penetratin translocates across a bilayer, a transmembrane water pore is formed instead [21]. The free energy barrier for translocation was found to be ~60 kJ/mol, even in the presence of the pore. While this theoretical value suggests direct translocation of penetratin is unlikely, the published *in vitro* experimental studies have yielded mixed results.

A fluorescence spectroscopy study by Thorén *et al*. concluded that penetratin can rapidly permeate a GUV without inducing a membrane pore [31]. In contrast, fluorescence experiments by Drin *et al*. found that penetratin could not permeate LUVs composed of 1-palmitoyl-2-oleoyl-*sn*-glycero-3-phosphocholine (POPC) (70 mol%) and anionic 1-palmitoyl-2-oleoyl-*sn*-glycero-3-phosphoglycerol (POPG) (30 mol%) lipids [32]. A later study by Persson *et al*. argued that the conflicting findings could be attributed to the lipid vesicle size or membrane curvature [33]. Their confocal microscopy studies found that penetratin could not permeate an anionic LUV composed of 1, 2-dioleoyl-*sn*-glycero-3-phosphocholine (DOPC) (60 mol%) and 1, 2-dioleoyl-*sn*-glycero-3-phospho-(1'-*rac*-glycerol) (DOPG) (40 mol%) lipids, whereas it could permeate a GUV containing more than 20 mol% PE and phosphatidic acid (PA) lipids [33]. On the other hand, Bárány-Wallje *et al*. used GUVs composed of POPC (75 mol%) and POPG (25 mol%) lipids [34] and found no evidence of translocation by penetratin [34]. This suggests that penetratin is more sensitive to the lipid composition than the lipid vesicle size (or curvature). In this respect, the behavior of penetratin and TAT are similar. For example, TAT has been found to cause rapid leakage of small fluorescent probes from LUVs containing negatively charged bis(monoacylglycerol)phosphate (BMP) lipids [35], while substitution of BMP with PG significantly reduces the ability of TAT to cause leakage [35]. In addition, SAXS experiments have shown that penetratin behaves analogously to TAT in generating bi-continuous cubic lipid phases in PE-rich lipid membranes [15].

Aside from lipid composition, the relative peptide to lipid (or P: L) ratio, is another important factor influencing the membrane activity of penetratin. Isothermal titration calorimetry experiments have shown that penetratin can permeate an anionic DOPC/DOPG LUV when the peptide concentration exceeds a certain threshold value, which was interpreted in terms of an "electroporation-like" model [36]. According to this model, the accumulation of cationic penetratin on the outer leaflet of the anionic

lipid vesicle causes a local transmembrane electric field. Above the threshold peptide concentration, the local electric field is strong enough to generate a pore via an electroporation-like mechanism. However, this model was challenged by solid-state NMR paramagnetic relaxation studies, which revealed that penetratin actually distributes on the inner leaflet as well, at even low peptide concentration [37]. The NMR studies suggest that the membrane permeation of penetratin could be attributed to a deep partitioning of the peptide into the acyl chains of the lipid bilayer [37], similar to what is seen in some studies for TAT. As suggested for the TAT peptide earlier, electrostatic interactions between penetratin and phosphate groups in the distal leaflet may then be responsible for penetratin crossing the lipid bilayer. Conformational changes in penetratin have also been observed, as the concentration of membrane-bound peptide increases above a critical value [38,39]. At low concentrations, penetratin adopts the α-helix configuration, but above the threshold concentration one observes apparent nucleation and growth of a β-aggregate on the membrane surface, reminiscent of amyloidal peptides. The β-aggregate may cause damage to the membrane integrity by extracting lipid molecules from the bilayer [39].

Penetratin has also been found to induce membrane invaginations or tubes protruding towards the lipid vesicle interior [40]. This "physical endocytosis" mechanism is a result of the deep partitioning of penetratin into the lipid membrane, which significantly alters the internal membrane tension and membrane curvature. This mode of action of penetratin on the lipid membrane is reminiscent of the bacterial Shiga toxin [41].

2.3 Oligoarginine

The discovery of oligoarginine as a highly efficient molecular agent for drug delivery is attributed to the seminal work by the groups of Wender and Futaki. They identified the guanidinium cation as the key component responsible for the rapid membrane permeation of ARCPPs [42,43]. This discovery initiated

the rapid development of novel guanidinium-rich drug delivery carriers, which include: peptoids; carbamates; carbonates; carbohydrates, and dendrimers [44]. Here, we will focus on oligoarginine itself as questions still remain concerning the mechanism and important molecular determinants by which oligoarginine permeates lipid membranes.

Cellular uptake of cationic oligoarginine was found to be >100 fold more effective than TAT, whereas other cationic peptides; oligolysine, oligohistidine and oligoornithine were essentially inactive [43,45]. So it appears charge is not the sole factor when it comes to enhancing membrane permeation. This is one of the reasons why there has been a lot of work attempting to determine whether it is instead the interaction between the guanidinium ion and lipids that plays the key role. Wender and colleagues have proposed an "adaptive translocation" model for oligoarginine penetration, based on water/octanol partitioning experiments [46]. As illustrated in Figure 1, cationic oligoarginine in a biphasic water/octanol system will preferentially dissolve in the water phase. However, after addition of sodium laurate (laurate is an anionic fatty acid), a large percentage of oligoarginine transfers to the octanol. By contrast, oligoornithine will stay primarily in the water phase. Octanol has long been viewed as a lipid mimic and these partitioning experiments imply that oligoarginine is able to enter the cell membrane with the aid of anionic lipids. The dramatic difference between oligoarginine and oligoornithine is ascribed to the ability of guanidinium ions to form bidendate hydrogen bonds with the laurate anion. Alkylated guanidinium oligomers, on the other hand, have a reduced ability to form hydrogen bonds and do not partition into the octanol phase in the presence of sodium laurate [47]. In addition, it was also found that the membrane potential has a large impact on the cellular uptake of oligoarginine into Jurkat cells [47]. Sakai and Matile performed similar experiments to compare oligoarginine and oligolysine partitioning from water to chloroform [48]. They found that oligoarginine but not oligolysine can transfer from water to chloroform with the aid of amphiphilic anions [48]. The water/octanol

partitioning experiments were also conducted for TAT and penetratin peptides, both peptides were found to partition into the octanol phase with the aid of amphiphilic anions such as fatty acids and lipids [49,50]. The adaptive translocation process for oligoarginine has the following features (as depicted in Figure 2):

i) The oligoarginine adsorbs to the membrane surface where it can associate with abundant anionic membrane receptors or lipids.

ii) Complex aggregate forms involving the oligoarginine and perhaps several lipid molecules (represented as an inverse micelle in Figure 2).

iii) The less polar aggregate translates across the lipid bilayer, driven by the membrane potential.

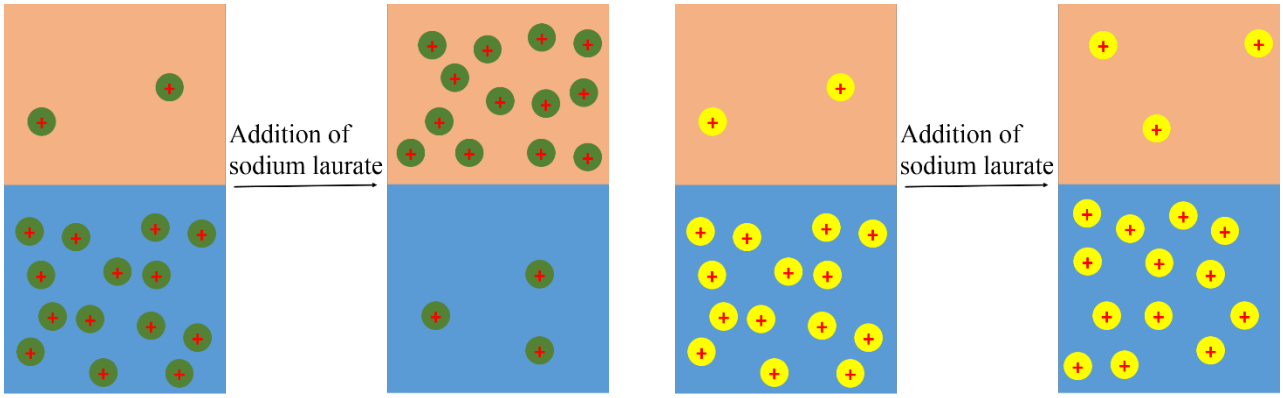

Figure 1. In the water-to-octanol partitioning experiments conducted by Rothbard et al.[47], both oligoarginine (A) and oligoornithine (B) were initially dissolved in water (colored blue). After adding sodium laurate into the biphasic system, the oligoarginine was found to partition into the octanol (colored orange) whereas oligoornithine remained in the water.

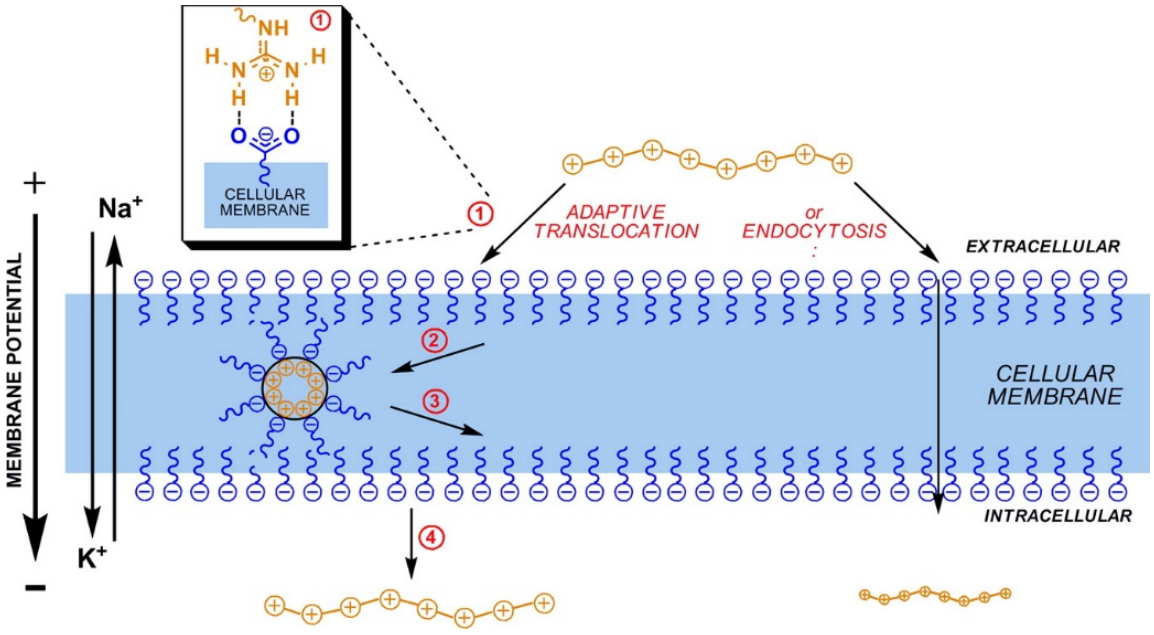

Figure 2. The adaptive translocation model for oligoarginine permeating through lipid bilayer. Oligoarginine can associate with anionic lipids to form an inverse micelle in the membrane. The inverse micelle then moves across the lipid bilayer due to the presence of transmembrane potential. The Figure is reproduced from reference [45].

The validity of using octanol to mimic the cell membrane interior has recently been questioned. Wet octanol saturates at ~20 mol% water which collects into nanoscale aggregates [51,52]. This suggests that water saturated octanol is actually not as hydrophobic as the membrane interior. It has also been noticed that the so-called Wimley-White octanol scales for amino acids correlate rather well with the Wimley-White membrane interfacial scales [53,54], which has led to the suggestion that the octanol scales reflect the partitioning of amino acids to the bilayer-water interface, rather than the membrane interior [55]. Likewise, the enhancement of water-to-octanol partitioning of ARCPPs due to amphiphilic anions mimics the increased binding affinity of ARCPPs to lipid bilayers containing anionic lipids. The differences in anion mediated partitioning observed between oligoarginine and other cationic peptides then reflects different interaction strengths with anionic lipids in the membrane [56].

SAXS experiments conducted by Wong and coworkers have revealed another difference between ARCPPs and oligolysine [15,57]. They showed that ARCPPs, including TAT, penetratin and oligoarginine, all induced the bi-continuous cubic phase in PE-rich lipid membranes. However, oligolysine instead induced an inverted hexagonal phase in similar membranes [15,57]. Wu *et al*. carried out all-atom and coarse-grained simulations, in an attempt to determine the molecular basis for the different actions of these peptides [58]. They found that while arginine and lysine amino acids have similar interactions with lipid phosphate groups, arginine interacts more strongly with lipid glycerols than lysine. The simulations showed that increased interactions with lipid glycerols led to the formation of a bi-continuous cubic lipid phase in the oligoarginine/lipid mixture [58]. Quantum mechanical calculations by Schmidt *et al*. gave a different explanation [59]. Their study showed that arginine can closely coordinate two phosphate groups (at 0.5 nm) with neighboring guanidinium ions stacking in a "face-to-face" orientation. By contrast, neighboring ammonium ions (on lysine) cannot get too close without large energetic penalties [59]. This suggests that arginine is more effective than lysine in coordinating lipids and inducing membrane curvature. The molecular origin of attraction between like-charged guanidinium ions has been investigated by Jungwirth and coworkers [60]. A recent MD simulation study by that group has found that oligoarginine can aggregate on an anionic lipid bilayer surface whereas oligolysine cannot [61].

Given its ability to permeate membranes, it is not surprising that oligoarginine is also associated with other structural changes in lipid bilayers. Hirose *et al*. discovered that deca-arginine (R10: R=arginine), attached to hydrophobic cargoes can stimulate the formation of "particle-like" multivesicular structures on the outer leaflet of the bilayer [62]. It was hypothesized that these multivesicular particles could facilitate the membrane permeation of oligoarginine. Maniti *et al*. reported similar results [63]. They found that nona-arginine (R9) and the amphipathic peptide sequence, RWRRWWRRW, (W=tryptophan)

induced budding and membrane tubulation on membrane surfaces. These tubes underwent rolling, so that multivesicular structures were formed [63]. While they are examples of membrane disruption, these structures are likely not part of the process for membrane permeation of oligoarginines. On the other hand, the formation of these membrane anomalies appears to result from surface area expansion on the outer leaflet of the membrane. Thus, these findings do provide evidence that oligoarginine peptides can expand the outer leaflet surface area and generate a membrane tension gradient through the bilayer, a property shared by other MAPs. MD simulations by Sun *et al*. have shown that adsorption of octaarginine (R8) onto a lipid bilayer can induce a surface tension of ~2.4 mN/m via membrane expansion [64]. Even a small percentage surface area increase can have large impact on a lipid membrane. For example, in a GUV with a diameter of 50 μm, the surface area expansion of the outer leaflet due to R8 adsorption would be ~ 6×10^8 nm^2 (estimated based on the simulations). A surface area expansion of this magnitude may cause significant changes in the membrane curvature and bring about budding or tube formation.

The observation of stable pores, due to adsorption of oligoarginine, has been reported in several experimental studies. Mishra *et al*. found that hexaarginine (R6) caused rupture of a PE-rich lipid membrane such that vesicle-trapped fluorescent dyes can be released [57]. Work by Herce *et al*. showed that R9 also induced small membrane pores. A transmembrane ionic current was induced in the peptide treated membranes by the application of an electric potential across the bilayer [65]. MD simulations by Huang and García calculated the free energy of cyclic R9 translocating across a lipid bilayer, both in the presence and absence of a transmembrane pore [66]. The presence of a pore lowers the free energy barrier to translocation by ~80 kJ/mol. Similar results were also reported in a coarse-grained simulation by Hu *et al* [67]. They observed that the translocation free energy barrier for a second R9 entering the lipid bilayer in the presence of an initial R9 restrained in the bilayer was significantly reduced,

suggesting cooperative and non-additive behavior of oligoarginine permeating through bilayer pores. Our own simulation work has revealed that membrane-bound oligoarginine peptides can significantly stabilize a water-filled membrane defect and facilitate its development into a membrane pore [64]. In that work, a membrane defect was initially created via lipid flip-flop, which was assumed to be associated with thermal fluctuations in the membrane. We suggest a new mechanism for oligoarginine translocation, wherein the peptide is able to recognize and stabilize a membrane defect and facilitate pore formation (via membrane expansion). Contiguous peptide translocation then follows if the adsorbed P: L ratio is large enough to allow continuous stabilization of the pore by entering (and leaving) peptides. As only a single peptide occupies the pore at any time, translocation occurs through pores small enough so as to not cause significant damage to the membrane.

The peptide length also seems to have a large impact on the membrane permeation of oligoarginines. Experiments by Futaki *et al*. showed that only oligoarginine peptides with 6-15 residues exhibited rapid membrane translocation [42]. The reason why peptide length is important remains poorly understood, but may be related to slower diffusion rates of longer peptide on the membrane surface. The geometry of oligoarginine seems also to be relevant. Cyclic analogues of oligoarginine and TAT have been found to permeate membranes more efficiently than their linear counterparts [68]. This was rationalized as an increase in the peptide structural rigidity due to the cyclization. In cyclic oligoarginine, the average distance between arginine residues is found to be larger compared to the more flexible linear oligoarginine. Experimental results reported by Wender and co-workers has found that increasing the spacing between the arginine residues in ARCPPs enhances their cellular uptake [69]. In the same vein, Walrant *et al*. reported that the chemical property of the spacer can also affect the membrane permeation ability of ARCPPs [70]. For example, the peptide, RRWWRRWRR, easily permeates cell membranes whereas RRLLRRLRR (L=leucine) shows no measurable permeability. These intriguing yet puzzling

results remain to be further investigated in order to better understand the membrane permeation behavior of ARCPPs.

2.4 Transportan 10

Tp10 (AGYLLGKINLKALAALAKKIL) is a 21-amino acid sequence amphipathic CPP. It is a synthetic peptide, derived by linking together (through a lysine, K) the 6-residue sequence from the neuropeptide galanin and the 14-residue sequence of the mastoparan antimicrobial peptide. Tp10 contains four cationic lysine residues but no arginine residue. The cationic residue content is only 19%, well below that of TAT (73%) and penetratin (44%). The relatively hydrophobic nature of tp10 suggests that this peptide has a likely different mode of action to other ARCPPs in the way they permeate and/or disrupt lipid membranes.

Almeida and coworkers have studied the action of tp 10 on LUVs composed of POPC (80 mol%) and POPS (20 mol%) lipids [71]. They have also proposed a kinetic model to explain their findings. According to this model, tp10 adsorbed on the outer leaflet of the LUV generates local curvature strains, which tend to perturb the lipid membrane. The membrane perturbation facilitates tp10 translocation across the membrane in order to relieve the membrane stress. Carboxyfluorescein (CF) fluorescent dyes, initially trapped in the LUVs, flow out through membrane pores induced by the tp10 translocation. The concentration difference of adsorbed peptide on inner and outer leaflets eventually becomes zero and pores close, ceasing dye leakage. This model is consistent with the observation that the tp10 induced so-called “graded release” of dyes from a collection of vesicles. In graded release kinetics, the internal dye concentration remains relatively homogeneous across all vesicles. Thus at around the half-life of the dye efflux process, most vesicles contain half the original amount of fluorescent dyes. Alternative efflux kinetics is the so-called “all-or-none” release which means that, during the efflux process, vesicles contain either all of the original amount of dye or are empty.

Yamazaki and coworkers proposed a different model, based on experiments with tp10 and a single GUV composed of DOPC (80 mol%) and DOPG (20 mol%) lipids [72]. They observed that tp10 translocation and membrane pore formation appear to be two independent processes. CF-labeled tp10 was found to rapidly translocate across the lipid bilayer, possibly via a mechanism similar to that suggested by Almeida *et al* [71]. However the pores, which allow this rapid translocation are small. A membrane pore, which is sufficiently large to allow passage of the Alexa Fluor 647 hydrazide (AF647) dye, only forms stochastically after tp10 peptides are distributed on both leaflets of the bilayer. Moreover, the size of the stochastic membrane pore is quite large, as ascertained by the use of the large dye, Texas Red-labeled Dextran 40K (with diameter of ~10 nm).

Further work is needed in order to explain these experimental findings. It is possible that tp10 is able to generate both small and large pores in a model membrane. The small pore is formed by peptide translocation, as the work by Almeida *et al.* has suggested, whereas a large pore could occur stochastically via rupture of the membrane tension produced by tp10 adsorption. On the other hand, equilibrium adsorption of peptide on both bilayer leaflets would imply the tension has been relieved. We have performed coarse-grained MD simulations on tp10 peptides in contact with a POPC bilayer [73]. We found that tp 10 is able to recognize a pre-ruptured membrane pore and stabilize it by diffusing to and aggregating at the pore edge [73]. Here, it is important to note that the reduced cationic residue content in tp10 may allow the peptide to aggregate with high local concentration at the pore edge.

In summary, we see that our understanding in the way that CPPs are able to penetrate lipid membranes is still incomplete. Much of the experimental evidence suggests that translocation is fairly rapid, yet the question of the high free energy barrier to direct penetration of sometimes highly charged cationic peptides still looms as an unresolved issue. There seems to be consensus that translocation through a (water filled) pore provides a lower free energy path, compared to a pore-less translocation.

There are many possible mechanisms for pore formation, we have explored two in our simulation studies: lipid flip-flop and direct peptide penetration (which has been shown to lead to pore formation in some force field models). By and large the free energy cost of forming a small pore by either of these methods appears to be roughly the same and both very large [64]. Explaining rapid translocation in the face of this free energy hurdle remains difficult. A promising hypothesis that has followed from our simulations is that translocation occurs through pores, in a cooperative fashion. That is, the initial formation of a pore may be a slow process (due to the large free energy barrier), but once it has formed, it remains stable, due to the translocation process itself. This idea has been explicitly explored in our recent simulation work, which showed that oligoarginine (R8) can stabilize pores by edge-adsorption, which then allows peptide to diffuse through the pores in a cooperative fashion, each translocating peptide keeping the pore stable for the following peptide. Of course this requires a suitably high adsorption density of peptides, the critical value we estimate to be approximately P:L ≈ 1:150 [64]. Coarse-grained simulations by Hu *et al* [67], support this mechanism, by showing translocation of an oligoarginine is enhanced by the presence of another in the pore. Thus the bottleneck to translocation is the rate of initial pore formation. However, even if pore formation is slow, the subsequent cooperative translocation may give an overall high rate of penetration. But does this really explain the observed rapid rate of translocation seen in experiments on CPPs? Perhaps there is more to the story. There is much evidence to suggest that the adsorption of peptide to the outer leaflet may well enhance the probability of pore formation in the first place, by the imposition of a surface tension gradient through the membrane. This enhancement of the rate of initial pore formation may well be needed to explain the overall rapid rate of translocation by CPPs. Finally, we see that in some cases, relatively large pores can also occur in these systems, after the translocation process has been initiated. Large pore formation seems to be driven by a combination of membrane weakening and large pore nucleation (via peptide

translocation) and increased surface tension (via peptide adsorption). That is, peptide adsorption increases surface tension, which then enhances rapid cooperative translocation, through the mechanisms discussed above. Translocation weakens the bilayer, introducing possible nucleating points for rupture of the membrane giving rise to large pores, again driven by the increased surface tension. In this context, it is worthwhile noting that some peptides seem to have an affinity to bilayer regions displaying negative Gaussian curvature, so they may act to stabilize thermally generated bilayer defects displaying this characteristic, even before they become full blown pores and hence catalyze pore formation by this process.

All of these processes also appear to be relevant to the mechanism of action of the next class of peptides we consider: antimicrobial peptides. However, in the case of antimicrobial peptides there appears to be an important role played by the peptides in stabilizing the large pores once they are formed. This will be discussed in the following section.

3. ANTIMICROBIAL PEPTIDES

Antimicrobial peptides are small proteins that are produced by virtually all living organisms on earth. In human bodies, antimicrobial peptides constitute an integral part of the innate immune system. They exhibit a broad spectrum of activity against bacteria, fungi, viruses and even cancer cells. In fact, antimicrobial peptides are now viewed as potent antibiotics and anti-cancer drugs. Unlike traditional antibiotics, which act by targeting specific membrane proteins, antimicrobial peptides usually cause microbial cell death by nonspecific disruption of cell membranes [74]. However, the testing of antimicrobial peptides in clinical trials has encountered difficulties, due mainly to their toxicity to healthy cells. The molecular processes by which antimicrobial peptides disrupt membranes are still not well established. Hence, the future development of safe and effective peptide-based antibiotics and

drugs will require more detailed experimental and theoretical studies of their mechanism of action against both eukaryotic and prokaryotic cell membranes.

Currently, more than 1,000 naturally occurring antimicrobial peptides have been identified. These peptides can be divided into three major categories on the basis of their secondary structure: α-helical, β-sheet and extended. Furthermore, most antimicrobial peptides are amphipathic, which means that they contain both cationic and hydrophobic residues. These common features lead us to believe that, to some extent, amphipathic antimicrobial peptides disrupt cell membranes through a common mechanism. Indeed, accumulating experimental and theoretical work has provided valuable information as to what those common actions may be.

3.1 Melittin

The 26-residue long melittin (GIGAVLKVLTTGLPALISWIKRKRQQ) peptide is the major component of the venom of the European honey bee *Apis mellifera* [75]. This peptide adopts a random coil conformation in solution but will quickly fold into an α-helix upon interacting with a lipid bilayer [76]. This conformational change upon membrane binding is a property shared by many other α-helical antimicrobial peptides. In the membrane-bound state, the α-helical melittin inserts deep into the lipid glycerol regions, most likely burying its hydrophobic residues while its α-helix is aligned parallel to the membrane plane [77]. Hence, high concentrations of membrane-bound melittin can cause significant perturbation of the outer leaflet, leading to area expansion and membrane thinning. These are precursor events, which presumably culminate in more drastic membrane disruption. Over the last few decades, a wealth of studies, using a variety of experimental techniques and model membrane systems have consistently reported that disruption of lipid membranes by melittin occurs via the generation of pores. However, researchers in the field are still vigorously debating the structures of these pores and the mechanisms by which they are formed and remain stable.

Reminiscent of mechanisms proposed for CPPs, Matsuzaki *et al.* have suggested that membrane pore formation by melittin is coupled with its translocation across the bilayer [78]. This is presumed to occur via membrane pores, which have a lifetime of milliseconds, consistent with graded efflux of vesicle-entrapped fluorescent dyes in kinetic experiments [78]. Notwithstanding its ability to explain experimental observations, this model has been critically questioned. Not least of the criticisms is the usual problem that the free energy cost for partitioning a cationic peptide like melittin (net charge is +5) from the bilayer surface to the bilayer interior is expected to be very large. As pointed out earlier, this free energy barrier is a major issue when it comes to determining translocation rates, so it is worthwhile exploring how these have been estimated in the literature. For example, according to several experimentally determined hydrophobicity scales, the free energy barrier to melittin translocation is in the range of 27-37 k_BT [53,79,80]. A free energy barrier of this magnitude essentially precludes direct penetration. This said, estimating free energy barriers to translocation using hydrophobicity scales can be somewhat misleading, especially for long peptides. Figure 3 illustrates a scenario depicting two possible pathways for melittin translocation. An estimate for the free energy barrier to translocation, based on hydrophobicity scales assumes a pathway much like is shown in Figure 3(A), *i.e.,* all residues have been totally inserted into the hydrophobic bilayer interior when the free energy is at (or near) its maximum. In actuality, the melittin may instead adopt a different configuration in order to reduce this barrier. In this context, it is worth noting that melittin contains five cationic residues, four of which are located near the C-terminus. So, as is illustrated in Figure 3(B), the melittin can initially insert its less polar N-terminus into the bilayer interior by adopting an orientation perpendicular to the membrane. In this way the C-terminus remains solvated for at least part of the translocation process. Irudayam *et al*. have performed umbrella sampling simulations and obtained a free energy cost of 22 k_BT for a single melittin to reorient itself from a membrane bound to a transmembrane state with an inserted N-terminus

inserted[81]. Strikingly, this free energy was reduced to 16 k_BT when the membrane-bound melittin concentration is high (P: L=1:32). This is at least 10 k_BT smaller than those predicted with the hydrophobicity scales. In support of the cooperative translocation model discussed with respect to CPPs, Irudayam *et al*. also report that the free energy of a second melittin to re-orient and insert its N-terminus across the bilayer deceases to 8.5 k_BT if another melittin has already inserted into the bilayer[81].

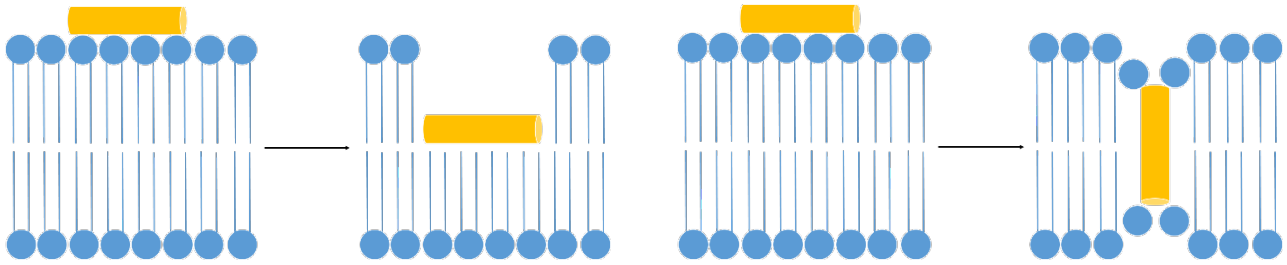

(A) (B)

Figure 3. Two possible pathways for a single melittin translocating across the lipid bilayer. In pathway (A), all residues are inserted into the bilayer interior in the intermediate step of the translocation process. In pathway (B), the peptide firstly re-orientates one end and then diffuses along the pore edge to reach the inner leaflet of the bilayer.

Direct translocation is not the only way that a cationic peptide could generate a membrane pore. Pore formation can also be enhanced by the action of increased surface tension. It has been postulated that melittin can form large and stable membrane pores by rupturing lipid membranes in this manner. A crucial mode of action of anti-microbial peptides is that they are able to stabilize these ruptured pores. Huang and co-workers have proposed a cooperative "two-state" model which incorporates such a mechanism [82]. According to this model, melittin initially adsorbs onto the outer leaflet of lipid bilayer with its α-helical axis parallel to the bilayer surface (S-state). The accumulation of melittin on the outer leaflet of lipid bilayer causes membrane thinning and internal membrane tension. Above a threshold concentration of melittin, the lipid membrane would be stochastically ruptured, due to the interplay

between membrane tension and the nucleation of a membrane defect. Simultaneously, a fraction of the membrane-bound melittin enters and adsorbs onto the pore edge. To do this they must reorient their axes so that they are perpendicular to the membrane surface (I-state). The resultant peptide-stabilized pore has an inner diameter of ~4 nm. As shown above, stable pores of particular size and life-time can be inferred by the persistent leakage of vesicle-entrapped fluorescent dyes. This mode of action of melittin is supported by dynamic tension spectroscopy experiments by Evans *et al.*, which showed that the threshold membrane tension for rupturing a lipid membrane is in the range of 2-35 mN/m, depending upon the lipid composition and the tension loading rate [83]. The membrane tensions generated by adsorbed melittin are within this range [84]. Furthermore, vesicle leakage assays by Wiedman *et al*. verified that melittin can generate pores by suddenly rupturing the lipid membrane [85]. A melittin concentration of P: L=1:100 was shown to induce an initial and rapid leakage of vesicle-entrapped fluorescent dyes, which then slowed to zero within ~10 minutes [85]. This result suggests a dynamic evolution of the membrane pore from an initially large size upon rupture, shrinking within minutes to a final state of either no pore, or one with a radius too small to allow passage of the dye. This behaviour was concentration dependent with dye efflux less than complete for concentrations less than P: L≈1:100 [85]. We have performed coarse-grained MD simulations on a range of amphipathic membrane active peptides, including melittin. Our results indicate that melittin has an affinity to a membrane pore (initially generated electrostatically in the simulations), absorbing to the inner surfaces of the pore and leading to pore stabilization in a concentration dependent manner [73]. We identified that this strong adsorption is driven by the exposure of hydrophobic lipid tails (in the highly curved bilayer of the pore) to the hydrophobic regions of the peptide. The final equilibrium size of the peptide-stabilized pore was found to increase with the peptide concentration.

Recent experimental work by Huang and co-workers has found that melittin peptides are already distributed on the inner leaflet of a lipid bilayer before the formation of large and stable membrane pores [86]. This intriguing finding suggests that melittin can induce both small (transient) and large (and stable) pores in a lipid membrane; a behavior similar to that of the CPP transportan 10, described above. This result may also help to reconcile the conflicting experimental results for melittin regarding the release kinetics of fluorescent dyes from vesicles [78,87,88].

Resolving the structure of pores with adsorbed melittin is an important step in determining how the peptide is able to stabilize them. Most published studies assert that melittin creates toroidal pores, characterized by outwardly arranged lipid heads (to give a negative Gaussian curvature) with the peptides oriented mainly perpendicularly with respect to the bilayer plane [89]. Remarkably, Huang and co-workers have obtained electron density maps of bromine labelled lipid heads in melittin lined lipid pores, using multiwavelength anomalous diffraction [86]. Their experiments indicate that melittin generates toroidal-shaped pores in the lipid membrane. Even so, questions still remain with respect to the number and the orientation of melittin peptides in the toroidal pore. Huang and co-workers reported that 4-7 perpendicularly orientated melittin are present in a stabilized pore with an inner diameter of ~4.4 nm [86]. However, recent all-atom MD simulations by us have found that the inner diameter of a membrane pore containing 4 melittin peptides is only about 1.5 nm (data not published). A possible reason for this discrepancy is that the melittin molecules lining the membrane pore are orientationally disordered, while the experiments measure the average projection of peptides in the direction perpendicular to the membrane plane [86]. This type of disordered structure was observed in our recent coarse-grained simulations [73], with pore sizes similar to what was seen in the experiments. Earlier atomistic MD simulations by Sengupta *et al.* [90] also report a so-called “disordered toroidal pore”.

However, the pores in that work were only ~1.5 nm in diameter and appear to be quite different to the large and stable pores identified in the experiments of by Huang and co-workers.

Lipid composition also has a large effect on the pore-forming ability of melittin. One surprising observation is that the addition of anionic lipids, like PG, into zwitterionic lipids significantly inhibits the membrane lytic power of melittin. For example, it has been reported that a threefold increase in melittin concentration is needed in order to obtain the equivalent efflux of fluorescent dyes from lipid vesicles containing anionic PG lipids, compared with vesicles made up of zwitterionic PC lipids only [88]. This experimental result is puzzling as the presence of anionic lipids in lipid bilayers should increase the concentration of melittin on the membrane surface. This has led some to postulate that melittin generates membrane pores in anionic lipid bilayers using a totally different mechanism. Ladokhin and White suggest that melittin disrupts anionic membranes through a "detergent-like" mechanism [91]. They propose that melittin peptides can aggregate on the membrane surface and this peptide aggregate will cause significant structural instabilities, literally disintegrating the bilayer. Another mechanism, suggested by van den Bogaart *et al*. is based on the hypothesis that melittin cannot insert deeply into the anionic lipid bilayers, but instead accumulates superficially on the membrane surface [92]. This accumulation of melittin eventually leads to aggregation of vesicles and fusion, accompanied by membrane pore formation.

3.2 Magainin 2

Magainins are a class of 23-residue long antimicrobial peptides isolated from the skin of the African clawed frog *Xenopus laevis* [93]. Magainin 2 (GIGKFLHSAKKFGKAFVGEIMNS) is the prototype antimicrobial peptide in the magainin family. In common with melittin, published studies have almost unanimously shown that magainin 2 can disrupt lipid membranes by generating membrane pores. However, unlike melittin, it appears that the activity of magainin 2 is highly sensitive to the lipid

composition of membranes. In particular, micromolar concentrations of magainin 2 can only permeate lipid membranes containing large fractions of anionic lipids, whereas equimolar magainin 2 has little disruptive effect on zwitterionic membranes [94]. It is known that bacteria and cancer cell membranes are rich in anionic lipids, whereas the outer leaflet of mammalian cell membranes are mainly composed of zwitterionic lipids and cholesterol. Hence, a complete understanding of the way magainin 2 interacts of with anionic and neutral membranes may prove very useful to the *de novo* design of novel antibiotics and anticancer drugs.

Notwithstanding this peptide's high specificity for anionic lipids, studies on model membranes have suggested that the underlying mechanisms by which magainin 2 induces membrane pores are similar to those of melittin. More specifically, magainin 2 appears to induce both small (transient) and large (stable) pores in anionic membranes. Matsuzaki and co-workers have reported on the small membrane pores induced by magainin 2 [95,96]. Their kinetic experiments studied the magainin 2 induced leakage of calcein from the (egg yolk) PC/PG LUV. They found that magainin 2 caused graded leakage from the anionic LUV, with a rate depending on the fourth or fifth power of the peptide concentration [95,96]. This result suggests that magainin 2 translocates into the inner leaflet of the lipid bilayer by forming a short-lived oligomeric pore containing four or five peptides. Matsuzaki *et al*. also reported that magainin 2 facilitated transmembrane lipid flip-flop [97]. This was attributed to the formation of a transient toroidal-shaped pore, which significantly lowers the free energy barrier for lipid flop-flop along the pore edge. This conclusion was reached after noting that magainin 2 facilitated lipid flip-flop at a rate similar to that of fluorescent dyes efflux from lipid vesicles. Significantly, magainin 2 was found to induce the concerted flip-flop of four different types of lipid, whose intrinsic flip-flop rates range from hours to days [97]. We note that melittin has also been reported to enhance lipid flip-flop rates [98]. However, a

thermodynamic study by Anglin *et al*. indicates that melittin facilitates lipid flip-flop by thinning the lipid bilayer, rather than by generating membrane pores [98].

Most studies have deduced that magainin 2 disrupts anionic membranes by generating large and stable pores. Ludtke *et al*. used neutron scattering to detect stable toroidal pores with an inner diameter of ~3 nm, induced in an anionic DMPC/DMPG (3:1) lipid membrane by magainin 2 [99]. Indeed the action of magainin 2 in anionic membranes is similar to that of melittin in zwitterionic membranes. Magainin 2 was found to cause membrane thinning before stable membrane pores were formed in a stochastic manner [99]. In addition, the pore only formed once a threshold peptide concentration was surpassed. The process seems to follow Huang's two-state model, which we described earlier. That is, membrane pore formation is accompanied by an orientation change of the magainin 2, from the S-state to the I-state, with concomitant stabilization of the membrane pore. Gregory *et al*. reported that magainin 2 induces all-or-none dye efflux from POPC/POPG (50:50) and POPC/POPG (70:30) LUVs [100].

Particularly noteworthy are the kinetic studies by Tamba *et al*., who investigated the activity of magainin 2 on a single anionic DOPC/DOPG (50:50) GUV [101]. They found that the efflux of smaller sized fluorescent dyes (Stokes-Einstein radius, R_{SE}<2.7 nm) occurs in two different stages: a transient and rapid leakage stage followed by a persistent and slow leakage stage. That is, once a pore is generated, all the entrapped smaller-sized fluorescent dyes would diffuse out of the GUV, consistent with an all-or-none mode of efflux kinetics. However, the leakage kinetics for larger sized fluorescent dyes (R_{SE}>3.6 nm) are quite different. It was shown that magainin 2 only induced partial leakage of the larger dyes. Hence, these results suggest that magainin 2 initially induces a large pore of some tens of nanometers in diameter in the anionic membrane. The large pore is not in equilibrium and it will quickly shrink within seconds to reach an equilibrium state with much smaller sized membrane pore. This observation is reminiscent of the behavior of melittin described earlier. It is also similar in spirit to

findings from experiments carried out by Brochard-Wyart and co-workers on GUVs [102]. They found that application of mechanical tension could rupture a giant lipid vesicle and form a large membrane pore of micrometer size. That large pore is also transient and completely reseals within seconds. The difference with pores induced by magainin 2 is that the peptide is able to stabilize the membrane pore, which they create. Pores, which are stabilized by magainin 2 in this way, can then allow persistent leakage of smaller sized vesicle-entrapped fluorescent dyes. However, the equilibrium pores will not be large enough to permit passage of the larger dyes. We note here that yet another membrane-active peptide, BAX5, derived from the apoptosis regulator BAX protein also induces membrane pores in a very similar way to magainin 2 [103]. That is, the initially induced membrane pore is large in size but dynamic, with the pore shrinking to an equilibrium state with much smaller size, stabilized by the peptide. Many other MAPs likely generate stable membrane pores in a similar fashion, but more experimental work is needed in order to verify this conjecture.

3.3 LL-37

LL-37 (LLGDFFRKSKEKIGKEFKRIVQRIKDFLRNLVPRTES) is a 37-residue long human antimicrobial peptide. It is derived from cathelicidin proteins, which play critical roles in the innate human immune defense system [104]. Like melittin and magainin 2, LL-37 is intrinsically unstructured in water but it readily adsorbs onto lipid membranes where it folds into α-helical form with the axis orientated parallel to the membrane plane. LL-37 is highly charged with 11 cationic residues and 5 anionic residues. Even so, NMR studies have shown that LL-37 inserts deeply into the hydrophobic acyl regions of the bilayer, where it causes significant structural perturbation and induces positive curvature in the lipid bilayer [105]. Though it inserts deep into the bilayer, the parallel orientation of the membrane-bound LL-37 is found to be unaltered. This has led to the conclusion that LL-37 disrupts lipid membranes by means of a “carpet mechanism” [106]. According to this mechanism, antimicrobial

peptides adsorb and accumulate on the outer leaflet of lipid bilayer to carpet the membrane. When the peptide concentration is sufficiently high they will disrupt the membrane in a detergent-like manner, eventually leading to the formation of micelles. However, work by Lee *et al*. has indicated that the predominately parallel orientation of LL-37 was likely a consequence of the small periodic (D) spacing of up to 5.2 nm in the model multilayer membranes [107]. This should be compared to the length of LL-37, which is ~5.5 nm. Using a swollen multilayer membrane instead (D spacing of ~7 nm), Lee *et al*. observed perpendicularly oriented LL-37 from oriented circular dichroism (OCD) measurements [107]. Importantly, the appearance in the spectrum of perpendicularly oriented peptide was coincident with large and stable pore formation in the membrane. Thus, the process by which LL-37 induces stable pores is likely akin to those of melittin and magainin 2, all of which seem to follow the two-state model.

Our coarse-grained MD simulations have revealed important features of the orientations of LL-37 in comparison to the shorter melittin and magainin 2 in membrane pores [73]. We found that the orientations of the three peptides (in α-helical form) were heterogeneous, which contradicts the assumption of perpendicular alignment used to fit the OCD data of Lee *et al* [86]. Wu *et al*. have also noted that, with respect to the interpretation of OCD spectra, it is not clear whether a particular result follows from a simple mix of parallel (S) and perpendicular (I) states of α-helical peptides or from tilted orientations [108]. Our simulations do provide plausible evidence that α-helical peptides in large membrane pores are not absolutely perpendicular [73]. Furthermore, we found that, while the tilt angle distributions of melittin and magainin 2 span a large range, LL-37 peptides in the pore are orientated more parallel to the membrane plane. A similar orientation for long peptides (in this case the 189-residue Apo-A1 peptide) in a "double-belt" structure was observed in coarse-grained simulations by Vácha and Frenkel [109]. A more parallel orientation distribution is caused by the mismatch between the

bilayer thickness and a relatively longer peptide. The parallel orientation means that LL-37 creates an equilibrium pore with a larger diameter than shorter peptides.

3.4 Protegrin-1

The 18-residue long protegrin-1 (PG-1) (RGGRLCYCRRRFCVCVGR) is an arginine and cysteine-rich β-hairpin antimicrobial peptide, isolated from porcine leukocytes [110]. Two cysteine-cysteine disulfide bonds stabilize the β-hairpin of PG-1, which creates a rigid solution structure that does not undergo significant structural change upon adsorbing to lipid membranes. The amino acid sequence in PG-1 is quite interesting: six cationic arginine residues are concentrated on two separate ends of the folded peptide while the remaining parts of the peptide are mainly composed of hydrophobic residues (see Figure 4). The distribution of hydrophilic and hydrophobic residues may have a lot to do with this peptide's ability to disrupt membranes, which is also sensitive to the lipid composition. For example, PG-1 can readily disrupt model membranes containing anionic lipids (mimicking bacterial membranes) but has little effect on zwitterionic lipid membranes [111]. In this regard, PG-1 is similar to magainin 2.

As with the other AMPs reviewed here, PG-1 is believed to disrupt lipid membranes by generating membrane pores, but again, the pore formation mechanisms are not well resolved. X-ray diffraction and OCD experiments by Heller *et al*. indicate that membrane-bound PG-1 causes membrane thinning and that the peptide exhibits an orientational change from a membrane-adsorbed S state to a pore-bound I state, once a threshold peptide concentration is reached [112]. This suggests that the process of pore formation by PG-1 also follows Huang's two-state model. Hong and coworkers reported the first high-resolution structure of PG-1 in a membrane pore [111]. Their ^{1}H and ^{19}F spin diffusion NMR data showed that eight or ten PG-1 peptides self-assemble into a parallel $(NCCN)_n$ (n=4 or 5) oligomeric structure in an anionic lipid membrane pore, with an inner diameter of ~2.1 nm [111]. This oligomer was later observed in MD simulations by Langham *et al*. [113] and Jang *et al* [114]. Langham *et al*.

suggested that the PG-1 oligomer is aligned in a barrel-stave shaped membrane pore [113]. However, rotational-echo double resonance experiments showed only a small distance between the lipid heads and the Arg residues at both the β-turn and in the middle of the β-strand (less than 6.5 Å to the phosphorous atom of lipid head), implying a toroidal pore [115]. Based on simulations, Lazaridis *et al*. argued that the parallel $(NCNC)_n$ oligomeric structure is more stable and exhibits more favorable binding energy to a toroidal membrane pore than the parallel $(NCCN)_n$ oligomer [116]. Despite this controversy, it is noted that in both the parallel $(NCCN)_n$ and the parallel $(NCNC)_n$ multi-mers, many cationic Arg residues on the hairpin turns and the N- and C-termini would cluster around the pore rim. The clustered Arg may play important roles in stabilizing the toroidal membrane pore by strongly interacting with the lipid phosphate groups.

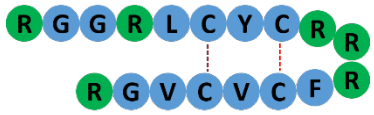

Figure 4. Amino acid distribution in the β-hairpin protegrin-1.

In this brief summary, we have seen that the experimental and simulation evidence implies a great deal of similarity between CPPs and AMPs, but also some crucial differences. In particular, AMPs seem to have a pronounced ability to stabilize large membrane pores, once they have formed. This action appears to be related to their amphipathic structure. In the final section below, we consider amyloid peptides. Here again we see some commonalities with CPPs and AMPs, in the sense that amyloidal peptides appear to compromise (specific) membrane types by stabilizing membrane pores. An area of significant difference, however, appears to be in the way that amyloidal peptides stabilize pores. This

seems to be connected with their ability to aggregate and form oligomeric and fibrillar structures. Remarkably, membranes appear to catalyze the formation of these peptide aggregates.

4. AMYLOID PEPTIDES

Amyloid peptides (and proteins) are characterized by their ability to form insoluble fibrillar aggregates containing highly ordered cross-β sheet structures. Amyloid peptides are intrinsically disordered in solution but may aggregate into fibrils following a transformation to a β-sheet conformation under pathological conditions. Amyloid peptides have attracted enormous attention from researchers because the extracellular depositions of amyloidal fibrils are now widely recognized to be intimately associated with the pathophysiology of a number of so-called amyloidal diseases. These include type II diabetes, Alzheimer's disease, and Parkinson's disease, to name just a few. Despite the huge body of work done in this area, the underlying factors which trigger amyloid formation and the mechanisms leading to cell death still remain unsolved. Accumulating evidence indicates that cell membranes could act as both the culprits and victims of the amyloid associated diseases [117]. On the one hand, a range of studies using model membrane systems has revealed that lipid membranes may facilitate the conformational change of amyloidal peptides and act as nucleation sites for fibril formation. On the other hand, peptide aggregation on membranes can lead to lipid disruption, possibly via several different pathways. Here, we review the proposed mechanisms of membrane disruption by two widely studied amyloid peptides: islet amyloid polypeptide (IAPP) and amyloid beta (Aβ) peptide.

4.1 IAPP

IAPP is a 37-residue long peptide hormone co-secreted with insulin by the islet β cells of the pancreas. The physiological functions of IAPP are not well established while the pathology of human type II diabetes mellitus is often characterized by the extracellular deposition of amyloids consisting of mainly

human IAPP (KCNTATCATQRLANFLV**H**SSNN**F**G**AI**L**SS**TNVGSNTY) and the associated death of human pancreatic β cells. However, many animals, e.g., rats, do not develop type II diabetes, which may be related to their native IAPP peptide. The amino acid sequence of rat IAPP is given as follows (KCNTATCATQRLANFLV**R**SSNN**L**G**PV**L**PP**TNVGSNTY) and is found to be non-amyloidogenic, due to the variation from human sequence (indicated in bold). It is also non-cytotoxic to rat pancreatic β cells [118]. Thus, it is proposed that human IAPP amyloid fibril is cytotoxic to human pancreatic β cells [119]. However, accumulating studies using model membranes later found that prefibrillar species, or IAPP oligomers, rather than the rigid fibrils, appear to be responsible for cell membrane disruption [120,121]. It is of interest to note that human IAPP and rat IAPP were found to differ significantly in their strength of interaction with lipid membranes despite the fact that the two peptides are different in only six residues [122].

Mirzabekov *et al*. made the first observation that human IAPP generated non-selective ion channels in a planar lipid bilayer, whereas comparable concentrations of rat IAPP did not [123]. In a biological context, the non-selectivity of ion channels would disrupt ionic homeostasis and cause cell death. Anguiano *et al*. found that the ion channels were induced by human IAPP oligomers but not by IAPP fibrils [124]. By contrast, ion channels were not seen in membranes interacting with rat IAPP, presumably because rat IAPP does not form oligomers either. Subsequent studies have further confirmed the pore-forming ability of human IAPP oligomers [125]. It is interesting to note that, recent work has shown that rat IAPP can generate pores in anionic lipid membranes [126]. This is an important finding as it suggests that membrane pore formation can occur independent of a peptides intrinsic ability to form fibrils, a conclusion also reached in studies by Brender *et al* [127]. They showed that the 37-residue long human IAPP can be divided into two functionally distinct regions: the 1-19 N-terminal region ($hIAPP_{1-19}$) is responsible for membrane pore formation whereas the amyloidogenic 20-29 region ($hIAPP_{20-29}$) forms

fibrils but is less disruptive to membranes than $hIAPP_{1-19}$ [127]. Despite this knowledge, the mechanism by which IAPP induces membrane pores is poorly understood, though it has been postulated that it may act in a way similar to AMPs [128]. Indeed IAPP does behave similarly to antimicrobial peptides in several respects:

i) Both IAPP and antimicrobial peptides are amphipathic and undergo a significant structural change (random coil to α-helix) upon adsorbing to lipid membranes.

ii) Adsorption of IAPP and antimicrobial peptides onto lipid membranes induces internal membrane tension and curvature strain. Though IAPP has been shown to induce negative membrane curvature [129], whereas most antimicrobial peptides mainly induce positive membrane curvature [106,130].

iii) Coarse-grained simulations by us have shown that both IAPP and antimicrobial peptides prefer to bind to the highly curved membrane pore edge and stabilize membrane pores [73].

iv) AMPs, like PG-1 and LL-37 have been reported to form fibrils under certain conditions [131,132].

A recent study by Last and Miranker proposes that IAPP and magainin 2 form membrane pores through a common mechanism [128]. However, it should be noted that the membrane pores induced by IAPP and antimicrobial peptides may be quite different in structure. In this context, we note that the antimicrobial peptide LL-37 and human IAPP both contain 37 residues and a high percentage of secondary structure in the adsorbed state, but LL-37 has a charge of +6 (five anionic and eleven cationic residues) whereas human IAPP contains only 2 cationic residues at pH=7. Our coarse-grained MD simulations have shown that the reduced electrostatic repulsion between IAPP allows it to aggregate at the edge of a large membrane pore, forming a stalk-like (prefibrillar) structure that stretches from the

pore edge into the solution [73]. On the other hand, LL-37 peptides were mainly adsorbed at the membrane pore edge.

Engel *et al*. measured the kinetics of calcein efflux from the DOPC/DOPS (70:30) LUVs, induced by human IAPP, as well as the rate of that peptide's fibril growth on the membrane surface [133]. They found that the two kinetic profiles were very similar, both being characterized by a lag phase of ~3 hours and the presence of a sigmoidal transition phase. More importantly, factors which are known to inhibit human IAPP fibril formation, also had an inhibitive effect on the efflux of calcein [133]. Their experimental studies thus suggest that the growth of fibrils is correlated with membrane disruption. However, calcein can only pass through membrane pores with inner diameters larger than 1.3 nm. This implies that small ion channels induced by human IAPP oligomers, which have been observed in many studies, may just not be large enough to allow the passage of calcein from the lipid vesicles. Thus, the connection between pore and fibril formation remains uncertain. Experiments by Cao *et al*. studied the interaction of human IAPP with pure (anionic) DOPG LUVs and observed that human IAPP oligomers can induce membrane pores allowing leakage of CF fluorescent dyes [134]. In addition, they found that fibril formation and elongation promote additional CF leakage from the DOPG vesicle, in agreement with the results of Engel *et al* [133]. So it appears that a complete understanding of the disruptive effect of human IAPP on membranes will likely combine both oligomers and fibril growth and their affect on membrane pore stabilization.

4.2 Aβ Peptide

Alzheimer's disease is an age-related neurodegenerative disorder. It is clinically characterized by the accumulation of extracellular senile plaques and intracellular neurofibrillary tangles in the brain. The major components of the extracellular senile plaques are Aβ peptides, which are produced by proteolytic cleavage of amyloid precursor protein (APP) by β- and γ-secretases at the C- and N-termini of the APP

[135]. The predominant forms of Aβ are the 40 residue-long $A\beta_{1\text{-}40,}$ which has the sequence (DAEFRHDSGYEVHHQKLVFFAEDVGSNKGAIIGLMVGGVV) and the 42 residue-long $A\beta_{1\text{-}42}$ with sequence (DAEFRHDSGYEVHHQKLVFFAEDVGSNKGAIIGLMVGGVVIA).

The mechanism by which Aβ peptides exert their neurotoxicity is also currently not well understood. However, studies using model membrane systems have provided evidence that Aβ peptides disrupt lipid membranes through a two-step process similar to that seen with IAPP. In particular, prefibrillar Aβ peptides have been reported to induce ion channels and pores in lipid membranes [125,136]. Of note, the ion channels induced by Aβ peptides are permeable to Ca^{2+} but not to Zn^{2+} [136]. In common with the mechanism described earlier, the channel induced by Aβ peptides is likely a consequence of the tension produced by adsorption onto the membranes. Micropipette aspiration experiments conducted by Ambroggio *et al*. showed that the exerted lysis tension to rupture a pure POPC GUV was ~8.2±0.1 mN/m whereas the required tension decreased dramatically to 0.3 mN/m when the lipid vesicle was mixed with $A\beta_{1\text{-}42}$ in the solution [137]. MD simulations by Jang *et al*. proposed two possible pathways for one pentamer of $A\beta_{17\text{-}42}$ reorienting and generating a pore in a lipid bilayer (see Figure 5) [138]. Their calculated potential of mean force (PMF) (using an implicit model) for the pentamer reorienting one end from the bilayer surface to the bilayer interior was ~14 kcal/mol for pathway 1 and ~9 kcal/mol for pathway 2. The PMF calculation results indicate that membrane pore formation induced by Aβ oligomers reorientation is very likely to occur within the time scale of minutes.

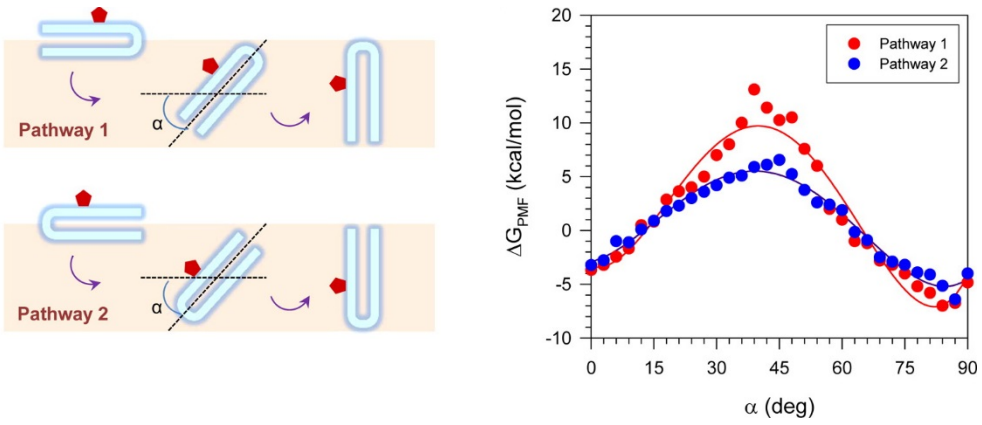

(A) (B)

Figure 5. (A) Two possible pathways for $A\beta_{17-42}$ pentamer re-orientation. Pathway 1 denotes the rotation of termini, while pathway 2 indicates the rotation of the bend. (B) The calculated PMF profiles for $A\beta_{17-42}$ pentamer re-orientating across the lipid bilayer. The reaction coordinate was chosen to be the insertion angle, α, for the two different rotation pathways. The Figures are reproduced from reference [138].

Work by Sciacca *et al*. found that nonspecific membrane fragmentation, induced by Aβ fibril growth, is highly dependent upon the presence of anionic gangliosides in the model membranes [139]. Gangliosides are particularly common in neuron cell membranes and it has been speculated that lipid rafts containing cholesterol and gangliosides are responsible for Aβ fibrillization [140]. In the two-step (channel formation and membrane fragmentation) model, an important question remains unanswered. That is whether there is a connection between membrane channel formation and amyloid fibrillization. In this regard, it is important to note that a *de novo* designed amphipathic antimicrobial peptide (KQKLAKLKAKLQKLKQKLAKL) initially generates a small pore in lipid membrane [141]. Intriguingly, this peptide continuously migrates to the pore edge and causes the membrane pore to expand in size (see Figure 6) [141]. It is not clear whether amyloid peptides also act to increase the size of pores via peptide aggregation, in this case prefibrillar oligomers and eventually fibrils. Future studies are needed to explore this possibility.

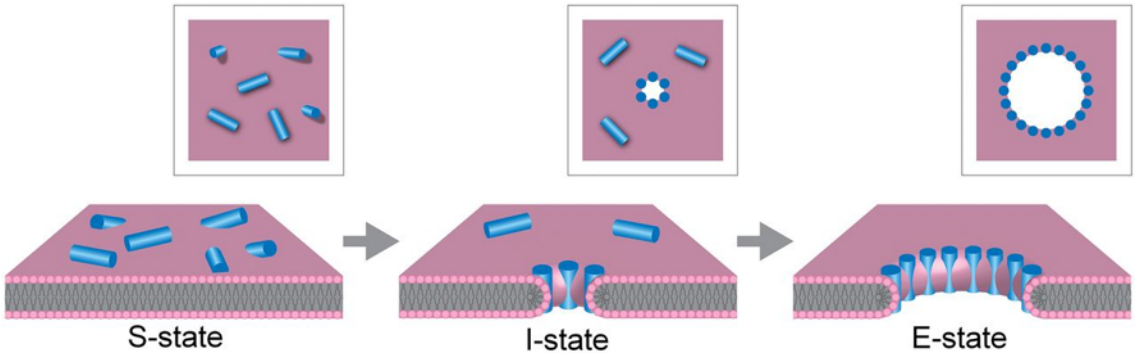

Figure 6. Three-state model proposed for an amphipathic antimicrobial peptide. In the I-state, a small number of peptides aggregate in the pore edge to stabilize a smaller-sized pore. In the E-state, the size of membrane pore is expanded as the amphipathic peptide continuously migrates from the membrane surface to the membrane pore edge. The Figure is reproduced from reference [141].

5. CONCLUSIONS

In this work, we reviewed the reported membrane permeation and disruption mechanisms for ten widely studied MAPs. Although these mechanisms were mainly derived from model membrane studies, they should also apply in the biological context, to the extent that model membranes adequately described real cell membranes. By summarizing the mechanisms of these peptides, we highlight the potentially common mode of actions of MAPs in the lipid membrane environment. All ten MAPs have been reported to induce pores in model membranes, though the size and lifetime of the pores appear to depend on the peptide species (and also lipid compositions). It is noted that a common pre-pore state is characterized by the deep embedding of peptides into the lipid bilayers. This causes membrane thinning and the generation of internal membrane tension. Membrane pore formation can be viewed as a process relieving the internal membrane tension. A critical property of MAPs is their ability to stabilize membrane pores (or defects). Without this action, a membrane pore would reseal almost instantaneously.

In the case of CPPs and AMPs rapid membrane translocation appears to be accompanied by small transient pores, whose formation is enhanced by asymmetric peptide adsorption. This translocation may primarily occur via cooperative diffusion, due to sequential stabilization of these small pores. There are possibly a number of ways in which this can be accomplished. Arginine-rich peptides appear to stabilize pores through the enhanced electrostatic interactions between guanidinium ions and the anionic lipid phosphate groups in a membrane pore environment with a relatively lower dielectric constant. On the other hand, amphipathic peptides may stabilize pores via interactions between hydrophobic residues and exposed lipid tails. The presence of these small pores and even peptide stabilized bilayer defects, together with a high membrane tension, means that membranes may rupture to form larger pores which, especially in the case of AMPs, are subsequently stabilized by the peptide. This leads to drastic compromise of the membrane and cell death. Amyloidal peptides also appear to act in a way to stabilize membrane pores. The way this occurs appears to be intrinsically linked to their ability to aggregate in fibrillar and prefibrillar structures. Indeed, there is evidence that prefibrillar oligomers are well able to stabilize small membrane pores, even before full-blown fibrils are nucleated. Our coarse-grained simulations appear to show in the case of human IAPP peptide, that a pore is able to act as a nucleating site for a prefibrillar structure. This suggests an intriguing cooperative, synergistic mechanism, whereby stochastic formation of pores (or even membrane defects) can act to enhance amyloidal peptide aggregation, which in turn stabilizes the pore (or catalyzes its formation from a defect), ultimately leading to a compromised membrane and cell death. Clearly, much work needs to be carried out in these systems before this or other mechanisms can be established. Theoretical studies employing molecular simulations can provide novel insights into the mechanisms by which MAPs interact with model lipid membranes. However, the limited size of simulation systems and the use semi-empirical force fields currently limit the accuracy of simulation results. Evaluating and comparing the current force fields used

in peptide-lipid simulations is both necessary and important to improve the reliability of simulations. Finally, one should be wary of various results that bespeak of artifacts associated with the setup of simulations, For example, it seems thermodynamically unlikely that cationic MAPs can quickly disrupt lipid bilayers within a few hundreds of nanoseconds.

Acknowledgement

Delin Sun performed the simulation work and wrote the substantial part of this review. Jan Forsman provided expert interpretation of the simulation work and provided scientific guidance to the project. Clifford Woodward provides expert interpretation and general supervision of the project and wrote a significant part of this review.

References

[1] Koller, D.; Lohner, K. The role of spontaneous lipid curvature in the interaction of interfacially active peptides with membranes. *Biochim. Biophys. Acta Biomembr.* **2014**, *1838*, 2250-2259.

[2] Matsuzaki, K. Physicochernical interactions of amyloid β-peptide with lipid bilayers. *Biochim. Biophys. Acta Biomembr.* **2007**, *1768*, 1935-1942.

[3] Teixeira, V.; Feio, M. J.; Bastos, M. Role of lipids in the interaction of antimicrobial peptides with membranes. *Prog. Lipid Res.* **2012**, *51*, 149-177.

[4] Peetla, C.; Stine, A.; Labhasetwar, V. Biophysical interactions with model lipid membranes: applications in drug discovery and drug delivery. *Mol. Pharm.* **2009**, *6*, 1264-1276.

[5] MacCallum, J.; Bennett, W. F. D.; Tieleman, D. P. Distribution of amino acids in a lipid bilayer from computer simulations. *Biophys. J.* **2008**, *94*, 3393-3404.

[6] Last, N. B.; Schlamadinger, D. E.; Miranker, A. D. A common landscape for membrane-active peptides. *Protein Sci.* **2013**, *22*, 870-882.

[7] Heitz, F.; Morris, M. C.; Divita, G. Twenty years of cell-penetrating peptides: from molecular mechanisms to therapeutics. *Br. J. Pharmacol.* **2009**, *157*, 195-206.

[8] Bolhassani, A. Potential efficacy of cell-penetrating peptides for nucleic acid and drug delivery in cancer. *Biochim. Biophys. Acta Rev. Canc.* **2011**, *1816*, 232-246.

[9] Medintz, I. L.; Pons, T.; Delehanty, J. B.; Susumu, K.; Brunel, F. M.; Dawson, P. E.; Mattoussi, H. Intracellular delivery of quantum dot-protein cargos mediated by cell penetrating peptides. *Bioconjug. Chem.* **2008**, *19*, 1785-1795.

[10] Vivès, E.; Brodin, P.; Lebleu, B. A truncated HIV-1 Tat protein basic domain rapidly translocates through the plasma membrane and accumulates in the cell nucleus. *J. Biol. Chem.* **1997**, *272*, 16010-16017.

[11] Richard, J. P.; Melikov, K.; Vivès, E.; Ramos, C.; Verbeure, B.; Gait, M. J.; Chernomordik, L. V.; Lebleu, B. Cell-penetrating peptides: a reevaluation of the mechanism of cellular uptake. *J. Biol. Chem.* **2003**, *278*, 585-590.

[12] Kaplan, I. M.; Wadia, J. S.; Dowdy, S. F. Cationic TAT peptide transduction domain enters cells by macropinocytosis. *J. Control Release.* **2005**, *102*, 247-253.

[13] Nakase, I.; Niwa, M.; Takeuchi, T.; Sonomura, K.; Kawabata, N.; Koike, Y.; Takehashi, M.; Tanaka, S.; Ueda, K.; Simpson, J. C. Cellular uptake of arginine-rich peptides: Roles for macropinocytosis and actin rearrangement. *Mol. Ther.* **2004**, *10*, 1011-1022.

[14] Duchardt, F.; Fotin-Mleczek, M.; Schwarz, H.; Fischer, R.; Brock, R. A comprehensive model for the cellular uptake of cationic cell-penetrating peptides. *Traffic* **2007**, *8*, 848-866.

[15] Mishra, A.; Gordon, V. D.; Yang, L. H.; Coridan, R.; Wong, G. C. L. HIV TAT forms pores in membranes by inducing saddle-splay curvature: Potential role of bidentate hydrogen bonding. *Angew. Chem. Int. Ed.* **2008**, *47*, 2986-2989.

[16] Wadhwani, P.; Epand, R. F.; Heidenreich, N.; Burck, J.; Ulrich, A. S.; Epand, R. M. Membrane-active peptides and the clustering of anionic lipids. *Biophys. J.* **2012**, *103*, 265-274.

[17] Ciobanasu, C.; Siebrasse, J. P.; Kubitscheck, U. Cell-penetrating HIV1 TAT peptides can generate pores in model membranes. *Biophys. J.* **2010**, *99*, 153-162.

[18] Piantavigna, S.; Abdelhamid, M. E.; Zhao, C.; Qu, X. H.; McCubbin, G. A.; Graham, B.; Spiccia, L.; O'Mullane, A. P.; Martin, L. L. Mechanistic details of the membrane perforation and passive translocation of TAT peptides. *ChemPlusChem* **2015**, *80*, 83-90.

[19] Choi, D.; Moon, J. H.; Kim, H.; Sung, B. J.; Kim, M. W.; Tae, G. Y.; Satija, S. K.; Akgun, B.; Yu, C. J.; Lee, H. W.; Lee, R. D.; Henderson, J. M.; Kwong, J. W.; Lam, K. L.; Lee, K. Y. C.; Shin, K. Insertion mechanism of cell-penetrating peptides into supported phospholipid membranes revealed by X-ray and neutron reflection. *Soft Matter* **2012**, *8*, 8294-8297.

[20] Herce, H. D.; García, A. E. Molecular dynamics simulations suggest a mechanism for translocation of the HIV-1 TAT peptide across lipid membranes. *Proc. Natl. Acad. Sci. U.S.A.* **2007**, *104*, 20805-20810.

[21] Yesylevskyy, S.; Marrink, S. J.; Mark, A. E. Alternative mechanisms for the interaction of the cell-penetrating peptides penetratin and the TAT peptide with lipid bilayers. *Biophys. J.* **2009**, *97*, 40-49.

[22] Akabori, K.; Huang, K.; Treece, B. W.; Jablin, M. S.; Maranville, B.; Woll, A.; Nagle, J. F.; García, A. E.; Tristram-Nagle, S. HIV-1 Tat membrane interactions probed using X-ray and neutron scattering, CD spectroscopy and MD simulations. *Biochim. Biophys. Acta Biomembr.* **2014**, *1838*, 3078-3087.

[23] Chen, X. C.; Sa'adedin, F.; Deme, B.; Rao, P. F.; Bradshaw, J. Insertion of TAT peptide and perturbation of negatively charged model phospholipid bilayer revealed by neutron diffraction. *Biochim. Biophys. Acta Biomembr.* **2013**, *1828*, 1982-1988.

[24] Su, Y.; Waring, A. J.; Ruchala, P.; Hong, M. Membrane-bound dynamic structure of an arginine-rich cell-penetrating peptide, the protein transduction domain of HIV TAT, from solid-state NMR. *Biochemistry* **2010**, *49*, 6009-6020.

[25] Derossi, D.; Joliot, A. H.; Chassaing, G.; Prochiantz, A. The third helix of the Antennapedia homeodomain translocates through biological membranes. *J. Biol. Chem.* **1994**, *269*, 10444-10450.

[26] Drin, G.; Cottin, S.; Blanc, E.; Rees, A. R.; Temsamani, J. Studies on the internalization mechanism of cationic cell-penetrating peptides. *J. Biol. Chem.* **2003**, *278*, 31192-31201.

[27] Letoha, T.; Gaál, S.; Somlai, C.; Czajlik, A.; Perczel, A.; Penke, B. Membrane translocation of penetratin and its derivatives in different cell lines. *J. Mol. Recognit.* **2003**, *16*, 272-279.

[28] Thorén, P. E. G.; Persson, D.; Isakson, P.; Goksör, M.; Onfelt, A.; Nordén, B. Uptake of analogs of penetratin, Tat(48-60) and oligoarginine in live cells. *Biochem. Biophys. Res. Commun.* **2003**, *307*, 100-107.

[29] Derossi, D.; Chassaing, G.; Prochiantz, A. Trojan peptides: the penetratin system for intracellular delivery. *Trends Cell Biol.* **1998**, *8*, 84-87.

[30] Kawamoto, S.; Takasu, M.; Miyakawa, T.; Morikawa, R.; Oda, T.; Futaki, S.; Nagao, H. Inverted micelle formation of cell-penetrating peptide studied by coarse-grained simulation: importance of attractive force between cell-penetrating peptides and lipid head group. *J. Chem. Phys.* **2011**, *134*, 095103.

[31] Thorén, P. E. G.; Persson, D.; Karlsson, M.; Nordén, B. The Antennapedia peptide penetratin translocates across lipid bilayers - the first direct observation. *FEBS Lett.* **2000**, *482*, 265-268.

[32] Drin, G.; Déméné, H.; Temsamani, J.; Brasseur, R. Translocation of the pAntp peptide and its amphipathic analogue AP-2AL. *Biochemistry* **2001**, *40*, 1824-1834.

[33] Persson, D.; Thorén, P. E. G.; Esbjörner, E. K.; Goksör, M.; Lincoln, P.; Nordén, B. Vesicle size-dependent translocation of penetratin analogs across lipid membranes. *Biochim. Biophys. Acta Biomembr.* **2004**, *1665*, 142-155.

[34] Bárány-Wallje, E.; S, K.; Serowy, S.; Geibel, S.; Pohl, P.; Bienert, M.; Dathe, M. A critical reassessment of penetratin translocation across lipid membranes. *Biophys. J.* **2005**, *89*, 2513-2521.

[35] Yang, S. T.; Zaitseva, E.; Chernomordik, L. V.; Melikov, K. Cell-penetrating peptide induces leaky fusion of liposomes containing late endosome-specific anionic lipid. *Biophys. J.* **2010**, *99*, 2525-2533.

[36] Binder, H.; Lindblom, G. Charge-dependent translocation of the trojan peptide penetratin across lipid membranes. *Biophys. J.* **2003**, *85*, 982-995.

[37] Su, Y.; Mani, R.; Hong, M. Asymmetric insertion of membrane proteins in lipid bilayers by solid-state NMR paramagnetic relaxation enhancement: a cell-penetrating peptide example. *J. Am. Chem. Soc.* **2008**, *130*, 8856-8864.

[38] Magzoub, M.; Kilk, K.; Eriksson, L. E. G.; Langel, Ü.; Gräslund, A. Interaction and structure induction of cell-penetrating peptides in the presence of phospholipid vesicles. *Biochim. Biophys. Acta Biomembr.* **2001**, *1512*, 77-89.

[39] Lee, C. C.; Sun, Y.; Huang, H. W. Membrane-mediated peptide conformation change from α-monomers to β-aggregates. *Biophys. J.* **2010**, *98*, 2236-2245.

[40] Lamazière, A.; Wolf, C.; Lambert, O.; Chassaing, G.; Trugnan, G.; Ayala-Sanmartin, J. The homeodomain derived peptide penetratin induces curvature of fluid membrane domains. *PLOS ONE* **2008**, *3*, e1938.

[41] Römer, W.; Berland, L.; Chambon, V.; Gaus, K.; Windschiegl, B.; Tenza, D.; Aly, M. R. E.; Fraisier, V.; Florent, J. C.; Perrais, D.; Lamaze, C.; Raposo, G.; Steinem, C.; Sens, P.; Bassereau, P.;

Johannes, L. Shiga toxin induces tubular membrane invaginations for its uptake into cells. *Nature* **2007**, *450*, 670-675.

[42] Futaki, S.; Suzuki, T.; Ohashi, W.; Yagami, T.; Tanaka, S.; Ueda, K.; Sugiura, Y. Arginine-rich peptides: an abundant source of membrane-permeable peptides having potential as carriers for intracellular protein delivery. *J. Biol. Chem.* **2001**, *276*, 5836-5840.

[43] Wender, P. A.; Mitchell, D. J.; Pattabiraman, K.; Pelkey, E. T.; Steinman, L.; Rothbard, J. B. The design, synthesis, and evaluation of molecules that enable or enhance cellular uptake: Peptoid molecular transporters. *Proc. Natl. Acad. Sci. U.S.A.* **2000**, *97*, 13003-13008.

[44] Stanzl, E. G.; Trantow, B. M.; Vargas, J. R.; Wender, P. A. Fifteen years of cell-penetrating, guanidinium-rich molecular transporters: basic science, research tools, and clinical applications. *Acc. Chem. Res.* **2013**, *46*, 2944-2954.

[45] Mitchell, D. J.; Kim, D. T.; Steinman, L.; Fathman, C. G.; Rothbard, J. B. Polyarginine enters cells more efficiently than other polycationic homopolymers. *J. Pept. Res.* **2000**, *56*, 318-325.

[46] Rothbard, J. B.; Jessop, T. C.; Wender, P. A. Adaptive translocation: the role of hydrogen bonding and membrane potential in the uptake of guanidinium-rich transporters into cells. *Adv. Drug Deliv. Rev.* **2005**, *57*, 495-504.

[47] Rothbard, J. B.; Jessop, T. C.; Lewis, R. S.; Muray, B. A.; Wender, P. A. Role of membrane potential and hydrogen bonding in the mechanism of translocation of guanidinium-rich peptides into cells. *J. Am. Chem. Soc.* **2004**, *126*, 9506-9507.

[48] Sakai, N.; Matile, S. Anion-mediated transfer of polyarginine across liquid and bilayer membranes. *J. Am. Chem. Soc.* **2003**, *125*, 14348-14356.

[49] Esbjörner, E. K.; Lincoln, P.; Nordén, B. Counterion-mediated membrane penetration: cationic cell-penetrating peptides overcome Born energy barrier by ion-pairing with phospholipids. *Biochim. Biophys. Acta Biomembr.* **2007**, *1768*, 1550-1558.

[50] Herce, H. D.; García, A. E.; Cardoso, M. C. Fundamental molecular mechanism for the cellular uptake of guanidinium-rich molecules. *J. Am. Chem. Soc.* **2014**, *136*, 17459-17467.

[51] Chen, B.; Siepmann, J. I. Microscopic structure and solvation in dry and wet octanol. *J. Phys. Chem. B* **2006**, *110*, 3555-3563.

[52] Sun, D. L.; Forsman, J.; Woodward, C. E. Evaluating force fields for the computational prediction of ionized arginine and lysine side-chains partitioning into lipid bilayers and octanol. *J. Chem. Theory Comput.* **2015,** *11*, 1775-1791.

[53] Wimley, W. C.; Creamer, T. P.; White, S. H. Solvation energies of amino acid side chains and backbone in a family of host-guest pentapeptides. *Biochemistry* **1996**, *35*, 5109-5124.

[54] Wimley, W. C.; White, S. H. Experimentally determined hydrophobicity scale for proteins at membrane interfaces. *Nat. Struct. Biol.* **1996**, *3*, 842-848.

[55] Roux, B. Lonely arginine seeks friendly environment. *J. Gen. Physiol.* **2007**, *130*, 233-236.

[56] Amand, H. L.; Boström, C. L.; Lincoln, P.; Nordén, B.; Esbjörner, E. K. Binding of cell-penetrating penetratin peptides to plasma membrane vesicles correlates directly with cellular uptake. *Biochim. Biophys. Acta Biomembr.* **2011**, *1808*, 1860-1867.

[57] Mishra, A.; Lai, G. H.; Schmidt, N. W.; Sun, V. Z.; Rodriguez, A. R.; Tong, R.; Tang, L.; Cheng, J. J.; Deming, T. J.; Kamei, D. T.; Wong, G. C. L. Translocation of HIV TAT peptide and analogues induced by multiplexed membrane and cytoskeletal interactions. *Proc. Natl. Acad. Sci. U.S.A.* **2011**, *108*, 16883-16888.

[58] Wu, Z.; Cui, Q.; Yethiraj, A. Why do arginine and lysine organize lipids differently? Insights from coarse-grained and atomistic simulations. *J. Phys. Chem. B* **2013**, *117*, 12145-12156.

[59] Schmidt, N. W.; Lis, M.; Zhao, K.; Lai, G. H.; Alexandrova, A. N.; Tew, G. N.; Wong, G. C. L. Molecular basis for nanoscopic membrane curvature generation from quantum mechanical models and synthetic transporter sequences. *J. Am. Chem. Soc.* **2012**, *134*, 19207-19216.

[60] Vondrášek, J.; Mason, P. E.; Heyda, J.; Collins, K. D.; Jungwirth, P. The molecular origin of like-charge arginine-arginine pairing in water. *J. Phys. Chem. B* **2009**, *113*, 9041-9045.

[61] Vazdar, M.; Wernersson, E.; Khabiri, M.; Cwiklik, L.; Jurkiewicz, P.; Hof, M.; Mann, E.; Kolusheva, S.; Jelinek, R.; Jungwirth, P. Aggregation of oligoarginines at phospholipid membranes: molecular dynamics simulations, time-dependent fluorescence shift, and biomimetic colorimetric assays. *J. Phys. Chem. B* **2013**, *117*, 11530-11540.

[62] Hirose, H.; Takeuchi, T.; Osakada, H.; Pujals, S.; Katayama, S.; Nakase, I.; Kobayashi, S.; T, H.; Futaki, S. Transient focal membrane deformation induced by arginine-rich peptides leads to their direct penetration into cells. *Mol. Ther.* **2012**, *20*, 984-993.

[63] Maniti, O.; Piao, H. R.; Ayala-Sanmartin, J. Basic cell penetrating peptides induce plasma membrane positive curvature, lipid domain separation and protein redistribution. *Int. J. Biochem. Cell Biol.* **2014**, *50*, 73-81.

[64] Sun, D. L.; Forsman, J.; Lund, M.; Woodward, C. E. Effect of arginine-rich cell penetrating peptides on membrane pore formation and life-times: a molecular simulation study. *Phys. Chem. Chem. Phys.* **2014**, *16*, 20785-20795.

[65] Herce, H. D.; García, A. E.; Litt, J.; Kane, R. S.; Martin, P.; Enrique, N.; Rebolledo, A.; Milesi, V. Arginine-rich peptides destabilize the plasma membrane, consistent with a pore formation translocation mechanism of cell-penetrating peptides. *Biophys. J.* **2009**, *97*, 1917-1925.

[66] Huang, K.; García, A. E. Free energy of translocating an arginine-rich cell-penetrating peptide across a lipid bilayer suggests pore formation. *Biophys. J.* **2013**, *104*, 412-420.

[67] Hu, Y.; Liu, X. R.; Sinha, S. K.; Patel, S. Translocation thermodynamics of linear and cyclic nonaarginine into model DPPC bilayer via coarse-grained molecular dynamics simulation: implications of pore formation and nonadditivity. *J. Phys. Chem. B* **2014**, *118*, 2670-2682.

[68] Lättig-Tünnemann, G.; Prinz, M.; Hoffmann, D.; Behlke, J.; Palm-Apergi, C.; Morano, I.; Herce, H. D.; Cardoso, M. C. Backbone rigidity and static presentation of guanidinium groups increases cellular uptake of arginine-rich cell-penetrating peptides. *Nat. Commun.* **2011**, *2*.

[69] Rothbard, J. B.; Kreider, E.; VanDeusen, C. L.; Wright, L.; Wylie, B. L.; Wender, P. A. Arginine-rich moleular transporters for drug delivery: role of backbone spacing in cellular uptake. *J. Med. Chem.* **2002**, *45*, 3612-3618.

[70] Walrant, A.; Vogel, A.; Correia, I.; Lequin, O.; Olausson, B. E. S.; Desbat, B.; Sagan, S.; Alves, I. D. Membrane interactions of two arginine-rich peptides with different cell internalization capacities. *Biochim. Biophys. Acta Biomembr.* **2012**, *1818*, 1755-1763.

[71] Yandek, L. E.; Pokorny, A.; Florén, A.; Knoelke, K.; Langel, Ü.; Almeida, P. F. F. Mechanism of the cell-penetrating peptide transportan 10 permeation of lipid bilayers. *Biophys. J.* **2007**, *92*, 2434-2444.

[72] Islam, M. Z.; Ariyama, H.; Alam, J. M.; Yamazaki, M. Entry of cell-penetrating peptide transportan 10 into a single vesicle by translocating across lipid membrane and its induced pores. *Biochemistry* **2014**, *53*, 386-396.

[73] Sun, D. L.; Forsman, J.; Woodward, C. E. Amphipathic membrane-active peptides recognize and stabilize ruptured membrane pores: exploring cause and effect with coarse-grained simulations. *Langmuir* **2015**, *31*, 752-761.

[74] Yeaman, M. R.; Yount, N. Y. Mechanisms of antimicrobial peptide action and resistance. *Pharmacol. Rev.* **2003**, *55*, 27-55.

[75] Raghuraman, H.; Chattopadhyay, A. Melittin: a membrane-active peptide with diverse functions. *Biosci. Rep.* **2007**, *27*, 189-223.

[76] Ladokhin, A. S.; White, S. H. Folding of amphipathic alpha-helices on membranes: energetics of helix formation by melittin. *J. Mol. Biol.* **1999**, *285*, 1363-1369.

[77] Hristova, K.; Dempsey, C. E.; White, S. H. Structure, location, and lipid perturbations of melittin at the membrane interface. *Biophys. J.* **2001**, *80*, 801-811.

[78] Matsuzaki, K.; Yoneyama, S.; Miyajima, K. Pore formation and translocation of melittin. *Biophys. J.* **1997**, *72*, 831-838.

[79] Hessa, T.; Kim, H.; Bihlmaier, K.; Lundin, C.; Boekel, J.; Andersson, H.; Nilsson, I.; White, S. H.; von Heijne, G. Recognition of transmembrane helices by the endoplasmic reticulum translocon. *Nature* **2005**, *433*, 377-381.

[80] Moon, C. P.; Fleming, K. G. Side-chain hydrophobicity scale derived from transmembrane protein folding into lipid bilayers. *Proc. Natl. Acad. Sci. U.S.A.* **2011**, *108*, 10174-10177.

[81] Irudayam, S. J.; Pobandt, T.; Berkowitz, M. L. Free energy barrier for melittin reorientation from a membrane-bound state to a transmembrane state. *J. Phys. Chem. B* **2013**, *117*, 13457-13463.

[82] Huang, H. W. Action of antimicrobial peptides: two-state model. *Biochemistry* **2000**, *39*, 8347-8352.

[83] Evans, E.; Heinrich, V.; Ludwig, F.; Rawicz, W. Dynamic tension spectroscopy and strength of biomembranes. *Biophys. J.* **2003**, *85*, 2342-2350.

[84] Lee, M. T.; Hung, W. C.; Chen, F. Y.; Huang, H. W. Mechanism and kinetics of pore formation in membranes by water-soluble amphipathic peptides. *Proc. Natl. Acad. Sci. U.S.A.* **2008**, *105*, 5087-5092.

[85] Wiedman, G.; Herman, K.; Searson, P.; Wimley, W. C.; Hristova, K. The electrical response of bilayers to the bee venom toxin melittin: evidence for transient bilayer permeabilization. *Biochim. Biophys. Acta Biomembr.* **2013**, *1828*, 1357-1364.

[86] Lee, M. T.; Sun, T. L.; Hung, W. C.; Huang, H. W. Process of inducing pores in membranes by melittin. *Proc. Natl. Acad. Sci. U.S.A.* **2013**, *110*, 14243-14248.

[87] Rex, S.; Schwarz, G. Quantitative studies on the melittin-induced leakage mechanism of lipid vesicles. *Biochemistry* **1998**, *37*, 2336-2345.

[88] Benachir, T.; Lafleur, M. Study of vesicle leakage induced by melittin. *Biochim. Biophys. Acta Biomembr.* **1995**, *1235*, 452-460.

[89] Yang, L.; Harroun, T. A.; Weiss, T. M.; Ding, L.; Huang, H. W. Barrel-stave model or toroidal model? A case study on melittin pores. *Biophys. J.* **2001**, *81*, 1475-1485.

[90] Sengupta, D.; Leontiadou, H.; Mark, A. E.; Marrink, S. J. Toroidal pores formed by antimicrobial peptides show significant disorder. *Biochim. Biophys. Acta Biomembr.* **2008**, *1778*, 2308-2317.

[91] Ladokhin, A. S.; White, S. H. 'Detergen-like' permeabilization of anionic lipid vesicles by melittin. *Biochim. Biophys. Acta Biomembr.* **2001**, *1514*, 253-260.

[92] van den Bogaart, G.; Mika, J. T.; Krasnikov, V.; Poolman, B. The lipid dependence of melittin action investigated by dual-color fluorescence burst analysis. *Biophys. J.* **2007**, *93*, 154-163.

[93] Zasloff, M. Magainins, a class of antimicrobial peptides from Xenopus skin: isolation, characterization of two active forms, and partial cDNA sequence of a precursor. *Proc. Natl. Acad. Sci. U.S.A.* **1987**, *84*, 5449-5453.

[94] Matsuzaki, K.; Sugishita, K.; Fujii, N.; Miyajima, K. Molecular basis for membrane selectivity of an antimicrobial peptide, magainin 2. *Biochemistry* **1995**, *34*, 3423-3429.

[95] Matsuzaki, K.; Murase, O.; Tokuda, H.; Funakoshi, S.; Fujii, N.; Miyajima, K. Orientational and aggregational states of magainin 2 in phospholipid bilayers. *Biochemistry* **1994**, *33*, 3342-3349.

[96] Matsuzaki, K.; Murase, O.; Miyajima, K. Kinetics of pore formation by an antimicrobial peptide, magainin 2, in phospholipid bilayers. *Biochemistry* **1995**, *34*, 12553-12559.

[97] Matsuzaki, K.; Murase, O.; Fujii, N.; Miyajima, K. An antimicrobial peptide, magainin 2, induced rapid flip-flop of phospholipids coupled with pore formation and peptide translocation. *Biochemistry* **1996**, *35*, 11361-11368.

[98] Anglin, T. C.; Brown, K. L.; Conboy, J. C. Phospholipid flip-flop modulated by transmembrane peptides WALP and melittin. *J. Struct. Biol.* **2009**, *168*, 37-52.

[99] Ludtke, S. J.; He, K.; Heller, W. T.; Harroun, T. A.; Yang, L.; Huang, H. W. Membrane pores induced by magainin. *Biochemistry* **1996**, *35*, 13723-13728.

[100] Gregory, S. M.; Pokorny, A.; Almeida, P. F. F. Magainin 2 revisited: a test of the quantitative model for the all-or-none permeabilization of phospholipid vesicles. *Biophys. J.* **2009**, *96*, 116-131.

[101] Tamba, Y.; Ariyama, H.; Levadny, V.; Yamazaki, M. Kinetic pathway of antimicrobial peptide magainin 2-induced pore formation in lipid membranes. *J. Phys. Chem. B* **2010**, *114*, 12018-12026.

[102] Karatekin, E.; Sandre, O.; Guitouni, H.; Borghi, N.; Puech, P. H.; Brochard-Wyart, F. Cascades of transient pores in giant vesicles: line tension and transport. *Biophys. J.* **2003**, *84*, 1734-1749.

[103] Fuertes, G.; García-Sáez, A. J.; Esteban-Martín, S.; Giménez, D.; Sánchez-Muñoz, O. L.; Schwille, P.; Salgado, J. Pores formed by Baxα5 relax to a smaller size and keep at equilibrium. *Biophys. J.* **2010**, *99*, 2917-2925.

[104] Dürr, U. H. N.; Sudheendra, U. S.; Ramamoorthy, A. LL-37, the only human member of the cathelicidin family of antimicrobial peptides. *Biochim. Biophys. Acta Biomembr.* **2006**, *1758*, 1408-1425.

[105] Henzler-Wildman, K. A.; Martinez, G. V.; Brown, M. F.; Ramamoorthy, A. Perturbation of the hydrophobic core of lipid bilayers by the human antimicrobial peptide LL-37. *Biochemistry* **2004**, *43*, 8459-8469.

[106] Henzler-Wildman, K. A.; Lee, D. K.; Ramamoorthy, A. Mechanism of lipid bilayer disruption by the human antimicrobial peptide, LL-37. *Biochemistry* **2003**, *42*, 6545-6558.

[107] Lee, C.; Sun, Y.; Qian, S.; Huang, H. W. Transmembrane pores formed by human antimicrobial peptide LL-37. *Biophys. J.* **2011**, *100*, 1688-1696.

[108] Wu, Y.; Huang, H. W.; Olah, G. A. Method of oriented circular dichroism. *Biophys. J.* **1990**, *57*, 797-806.

[109] Vácha, R.; Frenkel, D. Simulations suggest possible novel membrane pore structure. *Langmuir* **2014**, *30*, 1304-1310.

[110] Steinberg, D. A.; Hurst, M. A.; Fujii, C. A.; Kung, A. H.; Ho, J. F.; Cheng, F. C.; Loury, D. J.; Fiddes, J. C. Protegrin-1: a broad-spectrum, rapidly microbicidal peptide with in vivo activity. *Antimicrob. Agents Chemother.* **1997**, *41*, 1738-1742.

[111] Mani, R.; Cady, S. D.; Tang, M.; Waring, A. J.; Lehrer, R. I.; Hong, M. Membrane-dependent oligomeric structure and pore formation of a beta-hairpin antimicrobial peptide in lipid bilayers from solid-state NMR. *Proc. Natl. Acad. Sci. U.S.A.* **2006**, *103*, 16242-16247.

[112] Heller, W. T.; Waring, A. J.; Lehrer, R. I.; Huang, H. W. Multiple states of beta-sheet peptide protegrin in lipid bilayers. *Biochemistry* **1998**, *37*, 17331-17338.

[113] Langham, A. A.; Ahmad, A. S.; Kaznessis, Y. N. On the nature of antimicrobial activity: a model for protegrin-1 pores. *J. Am. Chem. Soc.* **2008**, *130*, 4338-4346.

[114] Jang, H.; Ma, B.; Lal, R.; Nussinov, R. Models of toxic beta-sheet channels of protegrin-1 suggest a common subunit organization motif shared with toxic Alzheimer beta-amyloid ion channels. *Biophys. J.* **2008**, *95*, 4631-4642.

[115] Tang, M.; Waring, A. J.; Hong, M. Phosphate-mediated arginine insertion into lipid membranes and pore formation by a cationic membrane peptide from solid-state NMR. *J. Am. Chem. Soc.* **2007**, *129*, 11438-11446.

[116] Lazaridis, T.; He, Y.; Prieto, L. Membrane interactions and pore formation by the antimicrobial peptide protegrin. *Biophys. J.* **2013**, *104*, 633-642.

[117] Kayed, R.; Sokolov, Y.; Edmonds, B.; Mclntire, T. M.; Milton, S. C.; Hall, J. E.; Glabe, C. G. Permeabilization of lipid bilayers is a common conformation-dependent activity of soluble amyloid oligomers in protein misfolding diseases. *J. Biol. Chem.* **2004**, *279*, 46363-46366.

[118] Nishi, M.; Chan, S. J.; Nagamatsu, S.; Bell, G. I.; Steiner, D. F. Conservation of the sequence of islet amyloid polypeptide in five mammals is consistent with its putative role as an islet hormone. *Proc. Natl. Acad. Sci. U.S.A.* **1989**, *86*, 5738-5742.

[119] Clark, A.; Cooper, G. J.; Lewis, C. E.; Morris, J. F.; Willis, A. C.; Reid, K. B.; Turner, R. C. Islet amyloid formed from diabetes-associated peptide may be pathogenic in type-2 diabetes. *Lancet* **1987**, *2*, 231-234.

[120] Gurlo, T.; Ryazantsev, S.; Huang, C. J.; Yeh, M. W.; Reber, H. A.; Hines, O. J.; O'Brien, T. D.; Glabe, C. G.; Butler, P. C. Evidence for proteotoxicity in beta cells in type 2 diabetes: toxic islet amyloid polypeptide oligomers form intracellularly in the secretory pathway. *Am. J. Pathol.* **2010**, *176*, 861-869.

[121] Ritzel, R. A.; Meier, J. J.; Lin, C. Y.; Veldhuis, J. D.; Butler, P. C. Human islet amyloid polypeptide oligomers disrupt cell coupling, induce apoptosis, and impair insulin secretion in isolated human islets. *Diabetes* **2007**, *56*, 65-71.

[122] Brender, J. R.; Hartman, K.; Reid, K. R.; Kennedy, R. T.; Ramamoorthy, A. A single mutation in the nonamyloidogenic region of islet amyloid polypeptide greatly reduces toxicity. *Biochemistry* **2008**, *47*, 12680-12688.

[123] Mirzabekov, T. A.; Lin, M. C.; Kagan, B. L. Pore formation by the cytotoxic islet amyloid peptide amylin. *J. Biol. Chem.* **1996**, *271*, 1988-1992.

[124] Anguiano, M.; Nowak, R. J.; Lansbury, P. T. Protofibrillar islet amyloid polypeptide permeabilizes synthetic vesicles by a pore-like mechanism that may be relevant to type II diabetes. *Biochemistry* **2002**, *41*, 11338-11343.

[125] Quist, A.; Doudevski, L.; Lin, H.; Azimova, R.; Ng, D.; Frangione, B.; Kagan, B.; Ghiso, J.; Lal, R. Amyloid ion channels: a common structural link for protein-misfolding disease. *Proc. Natl. Acad. Sci. U.S.A.* **2005**, *102*, 10427-10432.

[126] Knight, J. D.; Hebda, J. A.; Miranker, A. D. Conserved and cooperative assembly of membrane-bound alpha-helical states of islet amyloid polypeptide. *Biochemistry* **2006**, *45*, 9496-9508.

[127] Brender, J. R.; Lee, E. L.; Cavitt, M. A.; Gafni, A.; Steel, D. G.; Ramamoorthy, A. Amyloid fiber formation and membrane disruption are separate processes localized in two distinct regions of IAPP, the type-2-diabetes-related peptide. *J. Am. Chem. Soc.* **2008**, *130*, 6424-6429.

[128] Last, N. B.; Miranker, A. D. Common mechanism unites membrane poration by amyloid and antimicrobial peptides. *Proc. Natl. Acad. Sci. U.S.A.* **2013**, *110*, 6382-6387.

[129] Smith, P. E.; Brender, J. R.; Ramamoorthy, A. Induction of negative curvature as a mechanism of cell toxicity by amyloidogenic peptides: the case of islet amyloid polypeptide. *J. Am. Chem. Soc.* **2009**, *131*, 4470-4478.

[130] Matsuzaki, K.; Sugishita, K.; Ishibe, N.; Ueha, M.; Nakata, S.; Miyajima, K.; Epand, R. M. Relationship of membrane curvature to the formation of pores by magainin 2. *Biochemistry* **1998**, *37*, 11856-11863.

[131] Jang, H.; Arce, F. T.; Mustata, M.; Ramachandran, S.; Capone, R.; Nussinov, R.; Lal, R. Antimicrobial protegrin-1 forms amyloid-like fibrils with rapid kinetics suggesting a functional link. *Biophys. J.* **2011**, *100*, 1775-1783.

[132] Sood, R.; Domanov, Y.; Pietiäinen, M.; Kontinen, V. P.; Kinnunen, P. K. Binding of LL-37 to model biomembranes: insight into target vs host cell recognition. *Biochim. Biophys. Acta Biomembr.* **2008**, *1778*, 983-996.

[133] Engel, M. F. M.; Khemtemourian, L.; Kleijer, C. C.; Meeldijk, H. J. D.; Jacobs, J.; Verkleij, A. J.; de Kruijff, B.; Killian, J. A.; Hoeppener, J. W. M. Membrane damage by human islet amyloid polypeptide through fibril growth at the membrane. *Proc. Natl. Acad. Sci. U.S.A.* **2008**, *105*, 6033-6038.

[134] Cao, P.; Abedini, A.; Wang, H.; Tu, L. H.; Zhang, X.; Schmidt, A. M.; Raleigh, D. P. Islet amyloid polypeptide toxicity and membrane interactions. *Proc. Natl. Acad. Sci. U.S.A.* **2013**, *110*, 19279-19284.

[135] Williams, T. L.; Serpell, L. C. Membrane and surface interactions of Alzheimer's Aβ peptide--insights into the mechanism of cytotoxicity. *FEBS Lett.* **2011**, *278*, 3905-3917.

[136] Lin, H.; Bhatia, R.; Lal, R. Amyloid beta protein forms ion channels: implications for Alzheimer's disease pathophysiology. *FASEB J.* **2001**, *15*, 2433-2444.

[137] Ambroggio, E. E.; Kim, D. H.; Separovic, F.; Barrow, C. J.; Barnham, K. J.; Bagatolli, L. A.; Fidelio, G. D. Surface behavior and lipid interaction of Alzheimer β-amyloid peptide 1-42: a membrane-disrupting peptide. *Biophys. J.* **2005**, *88*, 2706-2713.

[138] Jang, H.; Connelly, L.; Arce, F. T.; Ramachandran, S.; Kagan, B.; Lal, R.; Nussinov, R. Mechanisms for the insertion of toxic, fibril-like β-amyloid oligomers into the membrane. *J. Chem. Theory Comput.* **2013**, *9*, 822-833.

[139] Sciacca, M. F.; Kotler, S. A.; Brender, J. R.; Chen, J.; Lee, D. K.; Ramamoorthy, A. Two-step mechanism of membrane disruption by Aβ through membrane fragmentation and pore formation. *Biophys. J.* **2012**, *103*, 702-710.

[140] Rushworth, J. V.; Hooper, N. M. Lipid rafts: linking Alzheimer's amyloid-β production, aggregation, and toxicity at neuronal membranes. *Int. J. Alzheimers Dis.* **2011**, *2011*, 603052.

[141] Rakowska, P. D.; Jiang, H.; Ray, S.; Pyne, A.; Lamarre, B.; Carr, M.; Judge, P.; Ravi, J.; Gerling, U. I. M.; Koksch, B.; Martyna, G. J.; Hoogenboom, B. W.; Watts, A.; Crain, J.; Grovenor, C. R. M.; Ryadnov, M. G. Nanoscale imaging reveals laterally expanding antimicrobial pores in lipid bilayers. *Proc. Natl. Acad. Sci. U.S.A.* **2013**, *110*, 8918-8923.